

# phantomlab

## Catphan<sup>®</sup> 700 Product Guide

Copyright © 2024

### WARRANTY

PHANTOM LABORATORY (“Seller”) warrants that this product shall remain in good working order and free of all material defects for a period of one (1) year following the date of purchase. If, prior to the expiration of the one (1) year warranty period, the product becomes defective, Buyer shall return the product to the Seller at:

By Truck  
Phantom Laboratory  
2727 State Route 29  
Greenwich, NY 12834

By Mail  
Phantom Laboratory  
PO Box 511  
Salem, NY 12865-0511

Seller shall, at Seller’s sole option, repair or replace the defective product. The Warranty does not cover damage to the product resulting from accident or misuse.

IF THE PRODUCT IS NOT IN GOOD WORKING ORDER AS WARRANTED, THE SOLE AND EXCLUSIVE REMEDY SHALL BE REPAIR OR REPLACEMENT, AT SELLER’S OPTION. IN NO EVENT SHALL SELLER BE LIABLE FOR ANY DAMAGES IN EXCESS OF THE PURCHASE PRICE OF THE PRODUCT. THIS LIMITATION APPLIES TO DAMAGES OF ANY KIND, INCLUDING, BUT NOT LIMITED TO, DIRECT OR INDIRECT DAMAGES, LOST PROFITS, OR OTHER SPECIAL, INCIDENTAL, OR CONSEQUENTIAL DAMAGES, WHETHER FOR BREACH OF CONTRACT, TORT OR OTHERWISE, OR WHETHER ARISING OUT OF THE USE OF OR INABILITY TO USE THE PRODUCT. ALL OTHER EXPRESS OR IMPLIED WARRANTIES, INCLUDING, BUT NOT LIMITED TO, THE IMPLIED WARRANTY OF MERCHANT ABILITY AND FITNESS FOR PARTICULAR PURPOSE, ARE HEREBY DISCLAIMED.

### WARNING

This product has an FH3-4 mm/min flame rating and is considered to be flammable. It is advised not to expose this product to open flame or high temperature (over 125° Celsius or 250° Fahrenheit) heating elements.

## CTP700

25-March-2024

## Medical device labeling

Manufactured by: Phantom Laboratory  
 2727 State Route 29  
 Greenwich, NY 12834 USA



EU Representative: Hoff & Lowendahl AB  
 Eudamed Actor ID: SE-AR-000001888  
 Address: Högåsvägen , 125 74141 Knivsta  
 Telephone number: +46 (0) 722313355  
 Email: info@lowendahl.eu



Product: Catphan® 700



Model: CTP700



UDI:



(01)00812266030048

Basic UDI: B-CTP700DZ

Device Class: 1



This device and its accessories are intended for use under direction of a trained medical physicist. Please refer to your machine manufacturer documentation and regulatory guidance for information on intended use.

A sample of this product has been assessed against the Essential Requirements of the EU Medical Device Regulation (MDR). The above mentioned product is deemed in compliance with MDR 2017/745 EU.

A risk assessment was conducted to the following standard: EN ISO14971  
 This declaration of conformity is the result of testing and evaluation performed by The Phantom Laboratory, Incorporated.

See next page for information on the Catphan® 710 Set and the included accessories. The Catphan® 710 Set includes the Catphan® 700 listed above.

Catphan®710 Set includes the Catphan®700 listed on the proceeding page and the following accessories which are listed with their individual UDI.

Product: Catphan® 710 Set

**REF** Model: CTP710

**UDI** UDI:



(01)00812266030055

Product: High Density Insert Set

**REF** Model: CTP748

**UDI** UDI:



(01)00812266030284

Product: 25-35cm oval OD 20cm thick uniformity material body annulus

**REF** Model: CTP579-20

**UDI** UDI:



(01)00812266030208

Product: 30-38cm oval OD 20cm thick uniformity material body annulus

**REF** Model: CTP651-20

**UDI** UDI:



(01)00812266030246

Product: 45° High resolution block with uniformity holder and mount

**REF** Model: CCT287

**UDI** UDI:



(01)00812266030307

Product: Scatter block extension for Catphan® 700

**REF** Model: CCT285

**UDI** UDI:



(01)00812266030314

# phantomlab

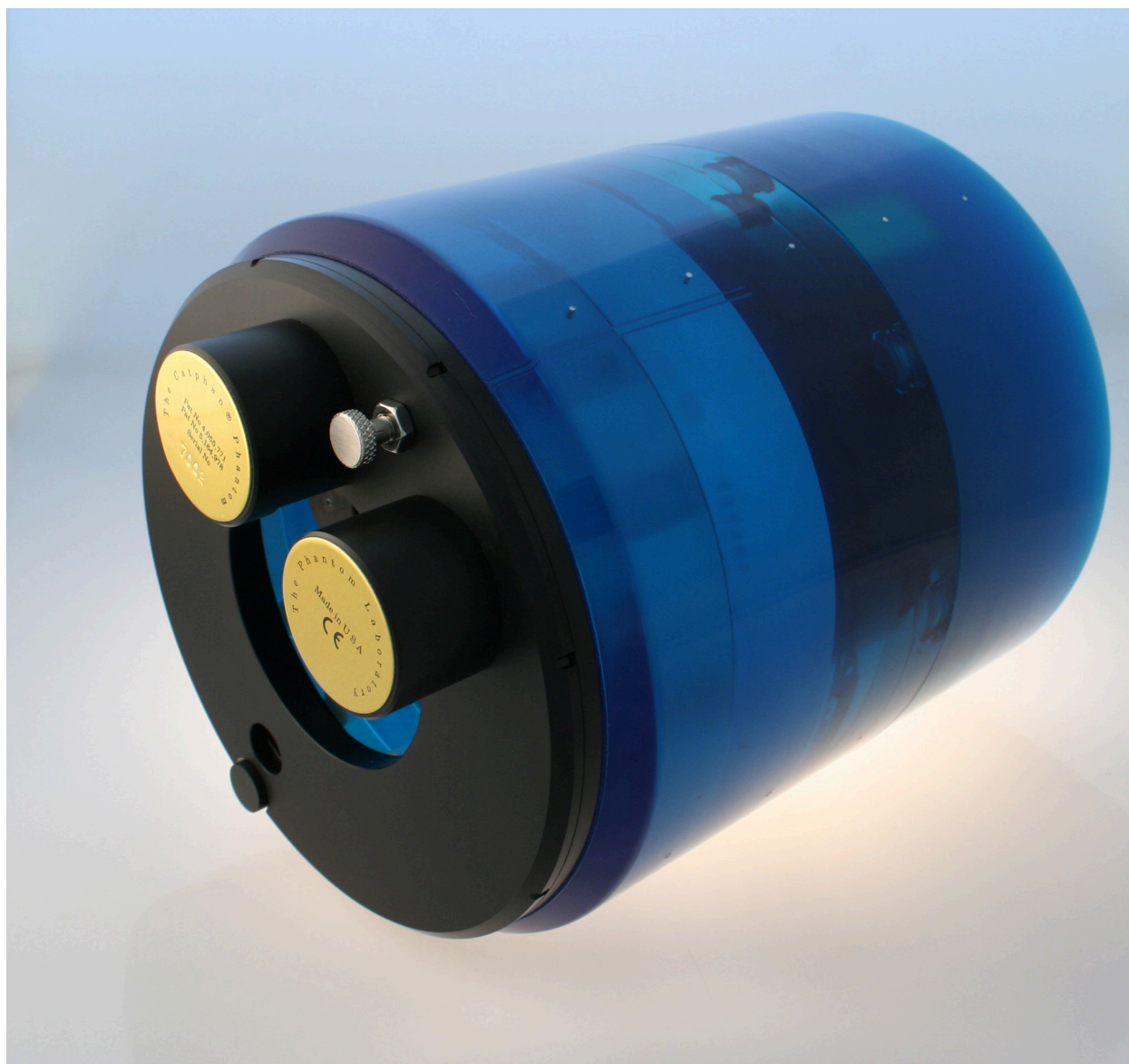
## Catphan® 700 and 710 set Product Guide Table of Contents

Warranty	1
Introduction	6
Multi-Slice CT by David Goodenough, Ph.D.	7
Initial phantom positioning	9
Illustration of the Catphan® 700 module positions	10
Incremental phantom modules positioning	10
Rotating the mount	11
Phantom position verification	12
CTP682 Geometry and Sensitometry module	13
Scan slice geometry (slice width)	14
Slice width measurement with wire ramps	15
Scan incrementation	16
Slice width measurement with bead ramps	17
Slice thickness from a profile of bead intensities	19
Additional methods for estimating and measuring slice thickness with bead ramps	20
Patient alignment system check	21
Circular symmetry of display system	22
Spatial linearity and pixel size verification	22
Bead or wire point source for point spread function and MTF	23
Use of automated scanner MTF programs	25
Bead point source for slice sensitivity profile	25
Spherical acrylic contrast targets	26
CT or Hounsfield Numbers by David Goodenough, Ph.D.	27
Sensitometry (CT number linearity)	28
Filling the water vial	29
CTP714 High resolution module with 1-30 line pair/cm gauges	30
CTP515 Low contrast module with supra-slice and subslice contrast targets	31
Wave ramp and bead modules	33
Background on the wave insert by David Goodenough, Ph.D.	34
CTP712 Image uniformity module	41
Smári analysis service	43



**Contents Continued**

Optional phantom annuli	44
Optional CCT285 Scatter extension	45
Optional CTP748 High Density Insert Set	47
Optional CCT287 45° High Resolution Phantom	48
Bibliography	49

**Catphan® 700**

**Introduction**

This product guide covers the Catphan® 700 and optional accessories, many which are included in the Catphan® 710 set

Phantom Laboratory and physicist, David J. Goodenough, Ph.D., are continually developing and researching new tests and modifications for the Catphan® phantoms. The test objects that make up the current Catphan® models embody more than a quarter century of scientific evaluation and field experience. This guide outlines the applications of each module contained in the Catphan® 700 phantoms.

We do not make specific recommendations on the content of your quality assurance program as each medical imaging facility has its own unique set of requirements. A sample program is provided to give you ideas for possible program content. We suggest a review of local governing regulations, manufacturers' specifications, and the needs of your radiologists and physicists before developing your CT quality assurance program.

If you have any additional questions please contact Phantom Laboratory at:  
Phone: 800-525-1190 or 518-692-1190  
email: [sales@phantomlab.com](mailto:sales@phantomlab.com)  
Additional product information is available at: [phantomlab.com](http://phantomlab.com)

## **Multi-Slice CT**

**by David J. Goodenough, Ph.D.**

At the request of Phantom Laboratory I have put together this summary for physicists who are familiar with CT image performance measurements and have not had experience with multi-slice CT scanners.

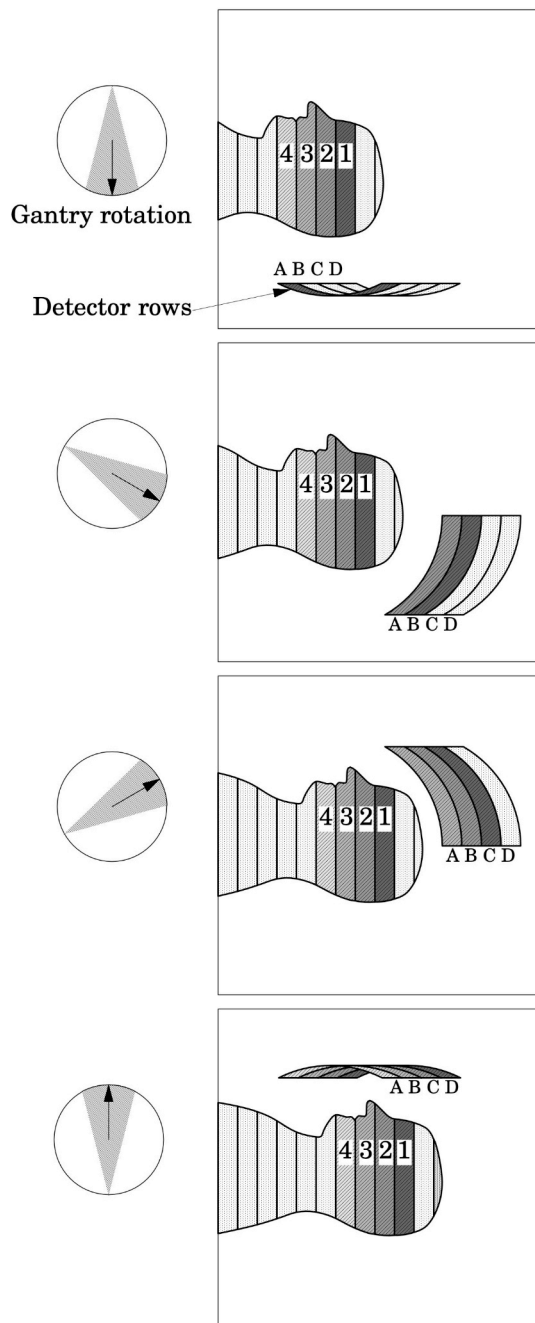
Multi-slice can use the same basic approach to image reconstruction as axial single slice CT. Each slice, or in some cases, the complete set of slices can be reconstructed from a “cone-beam” algorithm. This seems to correct the natural divergence from a single focal spot position to the detector position as positioned away from the control detector(s). Both modalities use the data from the detectors (positioned 360° around the patient) to reconstruct the axial patient images. The key difference between axial single slice CT and multi-slice is the axial image produced by single slice CT is developed from a single row of detectors, and the axial image made from a multi-slice scanner uses segments from several rows of detectors. With a multi-slice scan, as the patient moves through the gantry and the tube rotates around the patient, the detector rows utilized change as the patient and gantry move (see sketch on the next page).

Additional variables in reconstruction result as the patient slice moves from one row of detectors to the next and the scanner reconstructs the images based on weighted averages between the relevant rows. In this way, multi-slice CT is analogous to spiral or helical single slice CT, but where the reconstruction is obtained from the combined slices rather than the interpolation between the readings of a single moving slice. Now add in focal spot variables and a little scatter to define in more detail the challenges and variables included in the reconstruction of a multi-slice image.

Because in spiral mode each multi-slice image is reconstructed from an ensemble of data taken in different positions across the beam and from different detector rows, the overall image quality differences between images are minimal. In the spiral mode each slice represents data as seen from all detector rows in a sense a kind of averaging of detector row positions. However, if you use a multi-slice “step and shoot” or axial mode, where each of the slices may be created from a single detector row (or rows depending on the selected slice thickness) with a consistent collimation, the differences between the slices will be evident. Step and shoot mode in a multi-slice CT scanner is operated like a conventional axial scanner by imaging with a fixed table position and then moving the table to the next position before imaging the next section of the phantom with a fixed table position. For example, with a step and shoot 8 slice scan it is expected that the middle slice numbers 4 and 5 will have better uniformity than outer slice numbers 1 and 8 because of the scanner x-ray beam geometry. However, if 1 and 8 or 4 and 5 are not similar, this may indicate a problem with the scanner.

When assessing a scanner with a step and shoot mode, it is important to cover the full detector width with the selected test objects. If the test object is narrower than the slice, the table will need to be incremented between scanning sequences so the object can be scanned by all active rows of the detector.

I recommend scanning through the entire phantom using different multi-slice spiral protocols for performance evaluations, as well as using the step and shoot approach for the bead ramps where slice geometry and the MTF can be measured for each slice and uniformity section where the signal to noise and uniformity of each slice (detector row) can be evaluated.



This simplified illustration of a multi-slice sequence operating in spiral mode shows how the slices are reconstructed with information for different detector rows. The imaging sequence of the first selected slice (slice 1) of the patient begins when slice 1 moves over detector row A. As the tube continues to rotate and the patient continues to move through the gantry, slice 1 is picked up by the detectors in row B. At the same time slice 2, which was outside the detector view, is picked up by the detectors in row A. This sequence continues until the last selected region of the patient has passed through all the active detector rows.

## Initial Phantom Positioning

The Catphan® phantom is positioned in the CT scanner by mounting it on the case.

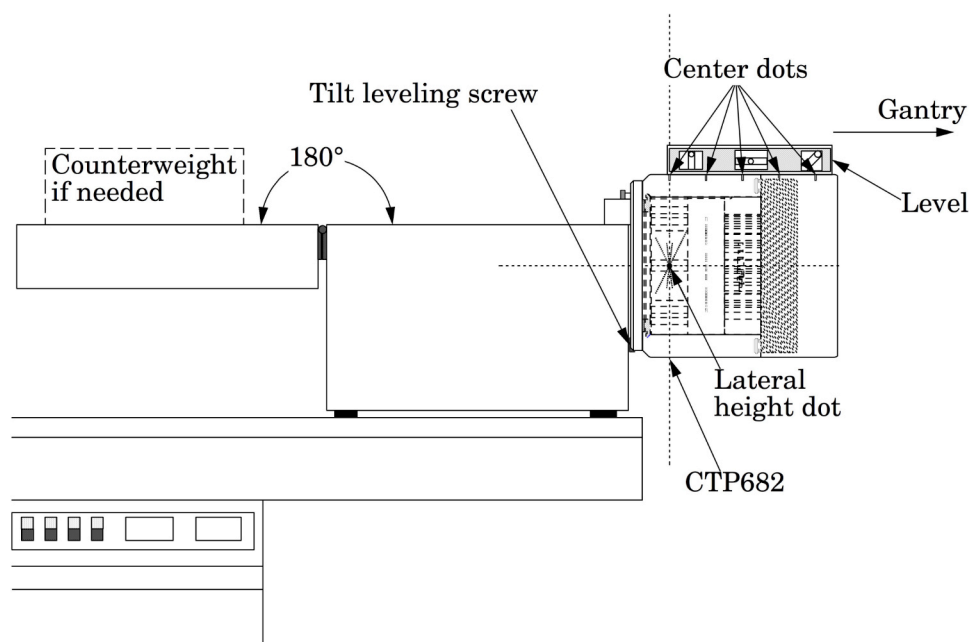
Place the phantom case on the gantry end of the table with the box hinges away from the gantry. It is best to place the box directly on the table and not on the table pads.

Open the box, rotating the lid back 180°. If you are using an annulus, additional weight will need to be placed in the box to counterweigh the phantom. The patient straps can be used for additional stability.

Remove the phantom from the box and hang the Catphan® from the gantry end of the box. Make sure the box is stable with the weight of the phantom and is adequately counterweighed to prevent tipping.

Use the tilt leveling screw to level the Catphan®. Once the phantom is level, slide the phantom along the end of the box to align the section center dots on the top of the phantom with the x-axis alignment light.

Use the table height and indexing drives to center the alignment dots on the side and top of the phantom's first section with the scanner alignment lights (CTP682 Geometry and Sensitometry module).

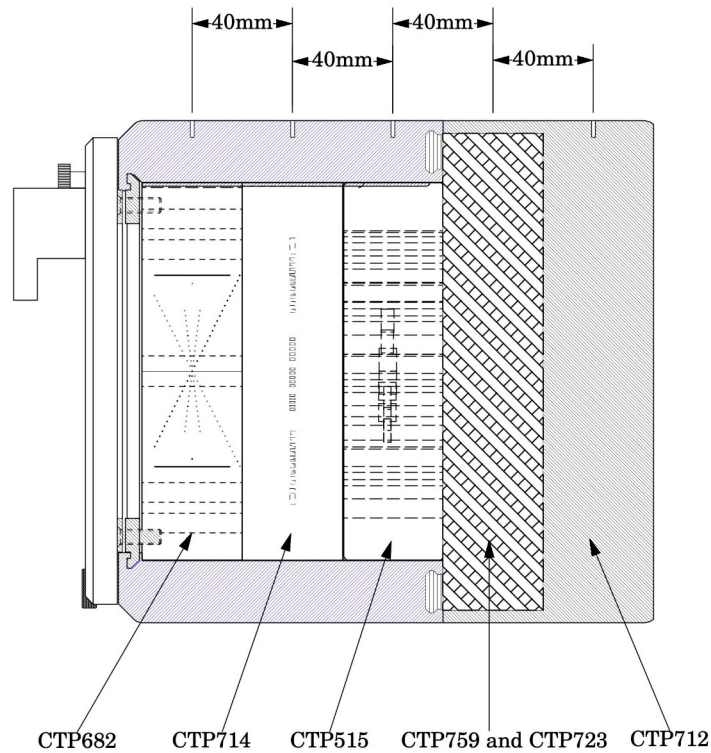


The z-axis scan alignment position can be selected from the localizer scan by centering the slice at the intersection of the crossed wire image created by the slice width ramps.

Scan the phantom and check the CTP682 module image for proper alignment as illustrated in the Phantom position verification section.

## Illustration of the Catphan® 700 module Positions

### Catphan® 700



### Incremental Phantom Module Positioning

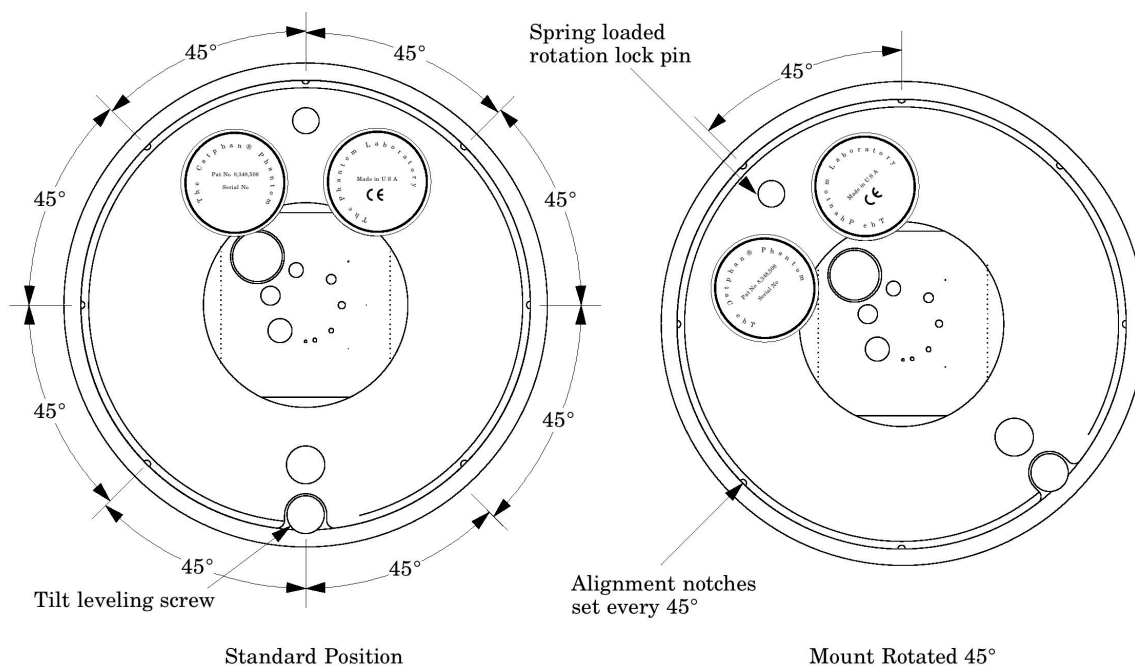
The Catphan® phantoms are designed so all test sections can be located by precisely indexing the table from the center of CTP682 to the center of each subsequent test module. This design eliminates the need to remount the phantom once the position of the CTP682 module has been verified. The indexing distances from the CTP682 module are listed below. Additional illustrations on the preceding page show the test modules and their index spacing. Phantom position verification is described on the next page.

Catphan® 700 test module locations:

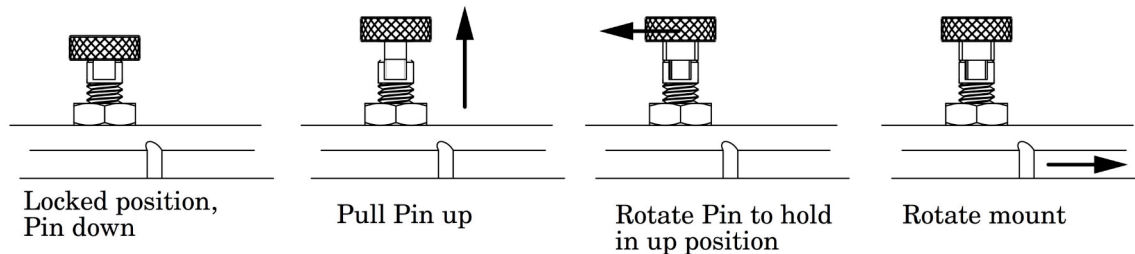
Module	Distance from center of CTP682
CTP682 Geometry, sensitometry module	0mm
CTP714 30 line pair high resolution	40mm
CTP515 Subslice and supra-slice low contrast	80mm
CTP759 Wave insert	120mm
CTP712 Solid image uniformity module	160mm



## Rotating the Mount



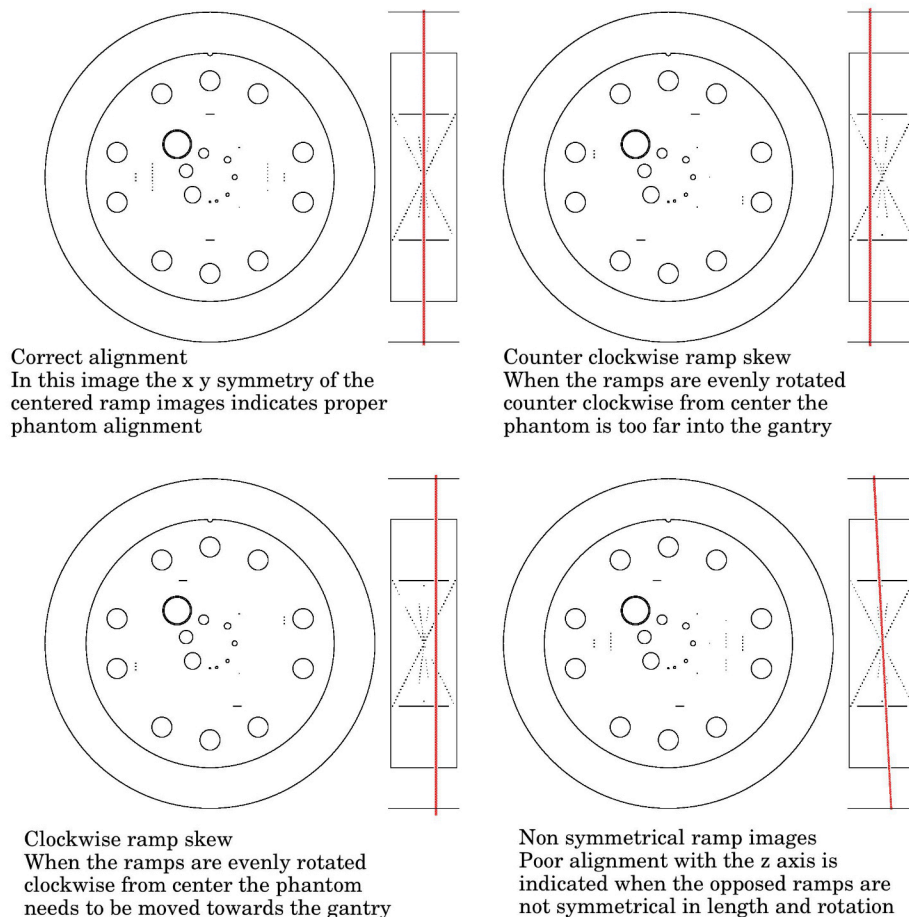
The Catphan® 700 has a mount that enables the phantom to be rotated around the z axis. This rotation enables the high-resolution gauges to be viewed with the pattern aligned parallel the x or y axis or rotated with respect to the x or y axis. There are 8 indexing holes located every 45° around the phantom.



The mount can be released from its position by pulling up on the Spring Loaded Rotation Lock Pin. By pulling up and rotating the pin it will be held in the “up” position as indicated in the sketch. Once the pin is in the “up” position the mount can be rotated. Once the correct location is obtained the pin can be rotated till it springs into the “down” position.

## Phantom Position Verification

By evaluating the scan image of CTP682 the phantom's position and alignment can be verified. The section contains 2 wire ramps which rise at 23° angles from the base to the top of the module and 2 pairs of bead ramps. The schematic sketches below indicate how the ramp images change if the scan center is above or below the z-axis center of the test module. The use of the scanner's grid image function may assist in evaluation of phantom position.



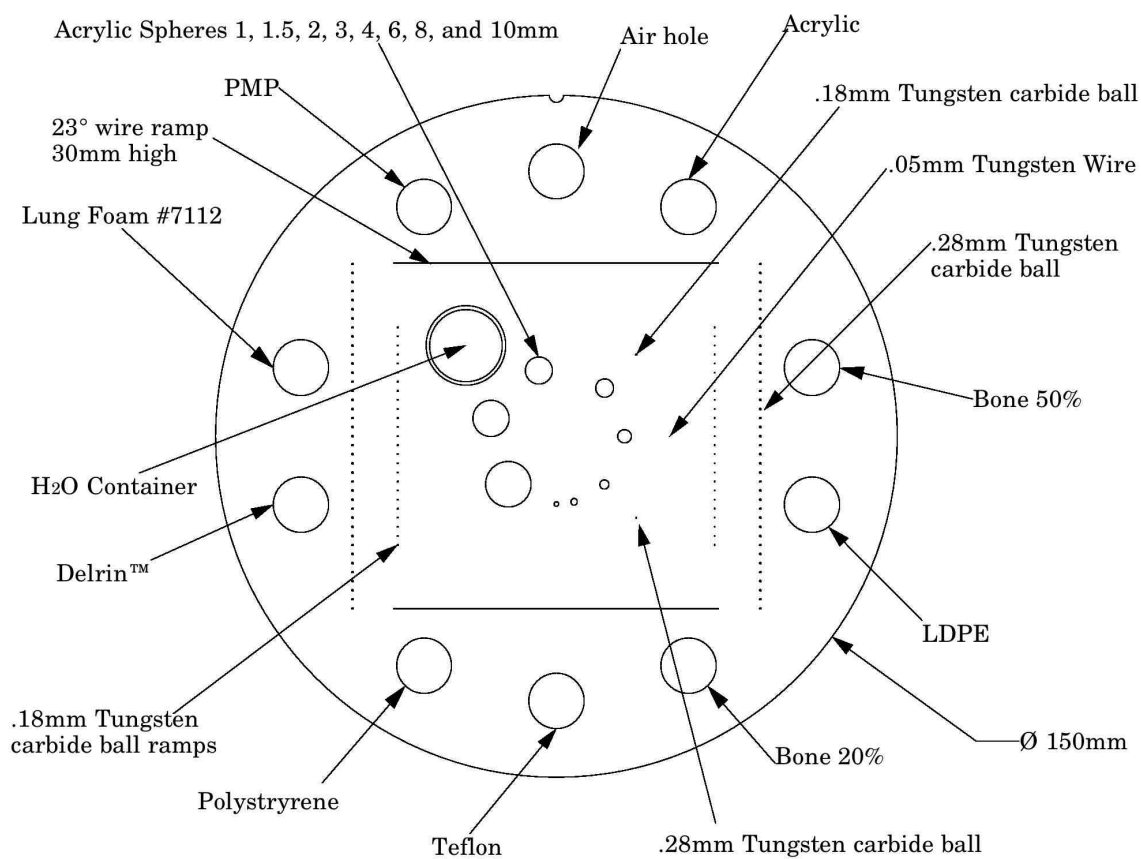
If misalignment is indicated by the scan image, the phantom should be repositioned to obtain proper alignment and then rescanned. If the images of the repositioned phantom duplicate the original misalignment indications, the scanner's alignment lights may require adjustment. See the Patient alignment system check section of this manual.

Once correct alignment has been established, you can proceed with the tests.



## CTP682 Geometry and Sensitometry Module

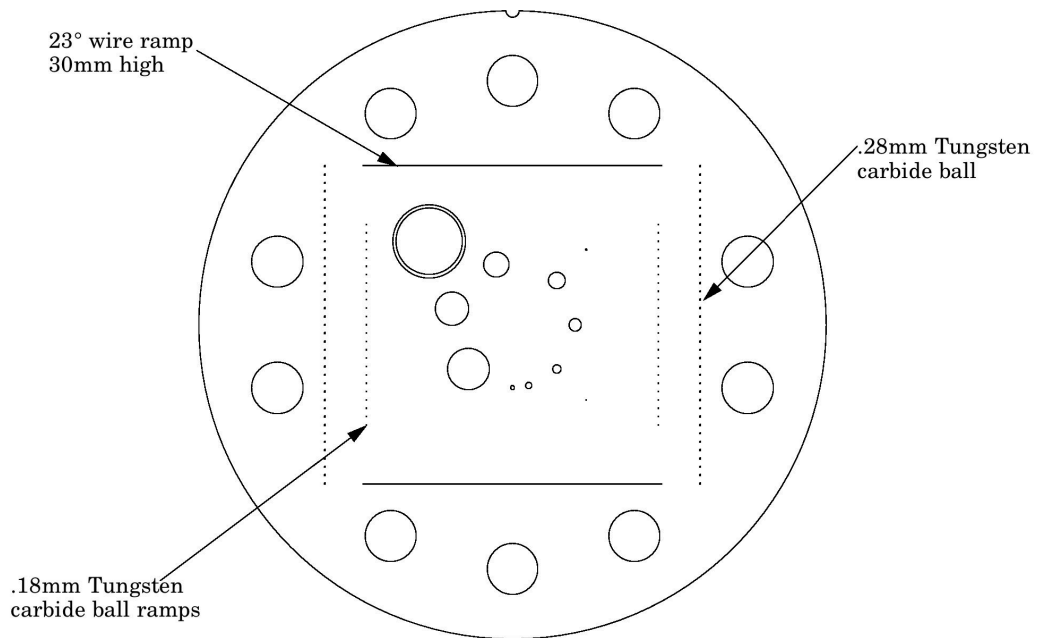
The CTP682 module is used for numerous measurements. The illustration below shows the different components. The following pages contain information on these components and their applications.



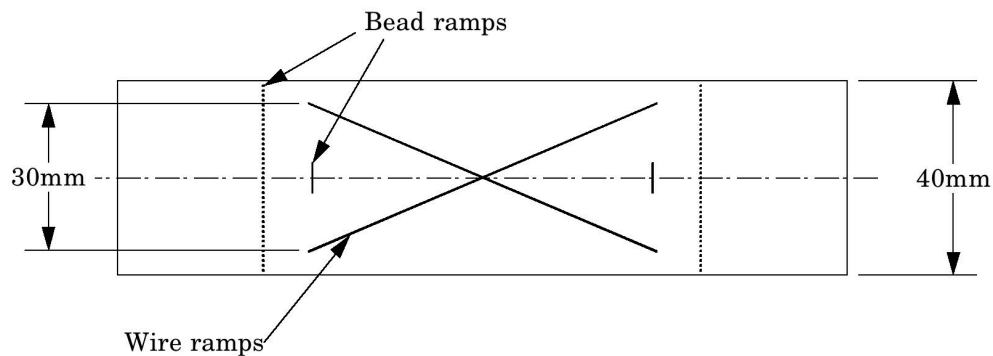
### Scan Slice Geometry (slice width)

The CTP682 module has a pair of  $23^\circ$  wire ramps oriented parallel to the x-axis at  $0^\circ$  rotation. These wire ramps are used to measure slice width, slice incrementation, and to check for misalignment errors as previously discussed. The use of these ramps for slice thickness and slice incrementation is discussed in the next section.

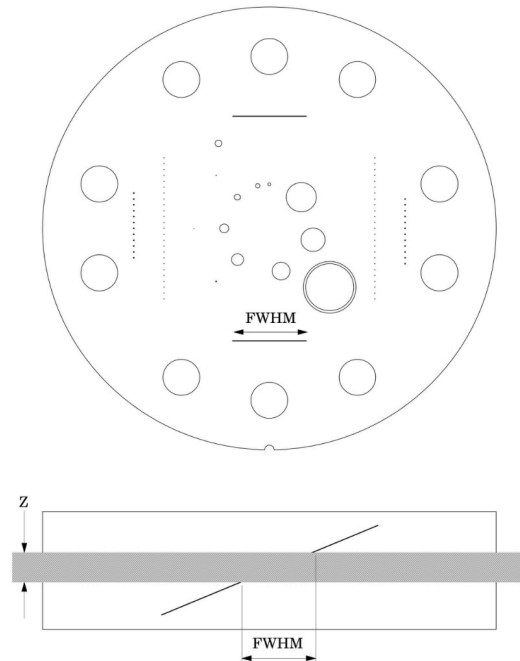
There are also two pairs of bead ramps aligned with the y-axis which, are discussed in the **Slice thickness measurement with bead ramps** section.



In the sketch below you can see the wire ramps which are positioned at  $23^\circ$  angles. You will see both ramps in the pair, which are crossing, in this side view.



## Slice Width Measurement with Wire Rams



The 23° wire ramp angle is chosen to improve measurement precision through the trigonometric enlargement of 2.38 in the x-y image plane.

To evaluate the slice width Z, measure the Full Width at Half Maximum (FWHM) length of any of the two wire ramps and multiply the length by 0.42:

$$Z = \text{FWHM} * 0.42$$

To find the FWHM of the wire from the scan image, determine the CT number values for the peak of the wire and for the background and calculate the 50% net peak.

To calculate the CT# peak of the wire, close down the CT “window” opening to 1 or the minimum setting and move the CT scanner “level” to the point where the ramp image just totally disappears. The CT number of the “level” at this position is your CT # peak.

The background CT number is measured near the ramp using the region of interest tool.

Using the above CT values, determine the half maximum:

First calculate the net peak... (CT # peak - background = net peak CT #)

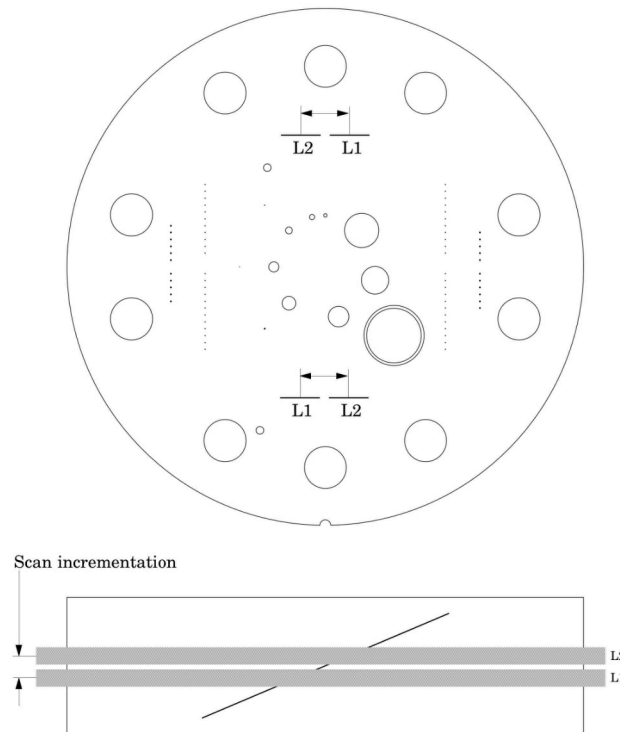
Calculate the 50% net peak... (net peak CT # ÷ 2 = 50% net peak CT #)

Calculate the half maximum CT number... (50% net peak CT # + background CT # = half max CT #)

Now that the half-maximum CT number has been determined, measure the full width at half maximum of the ramp. Set the CT scanner level at the half maximum CT value and set your window width at 1. Measure the length of the wire image to determine the FWHM. Multiply the FWHM by

0.42 to determine the slice width.

### Scan Incrementation



Schematic illustration above is of two sequential 5mm scans superimposed. L1 is the center point on the 23° ramp in the first scan image, and L2 is the center point on the 23° ramp on the second image.

Use the wire ramps to test for proper scanner incrementation between slices, and for table movement.

Scan section 1 using a given slice width, (e.g. 5mm). Increment the table one slice width (e.g. 5mm) and make a second scan. Establish the x and y coordinates for the center of each ramp image. Calculate the distance between these points and multiply by the 23° ramp angle correction factor of 0.42.

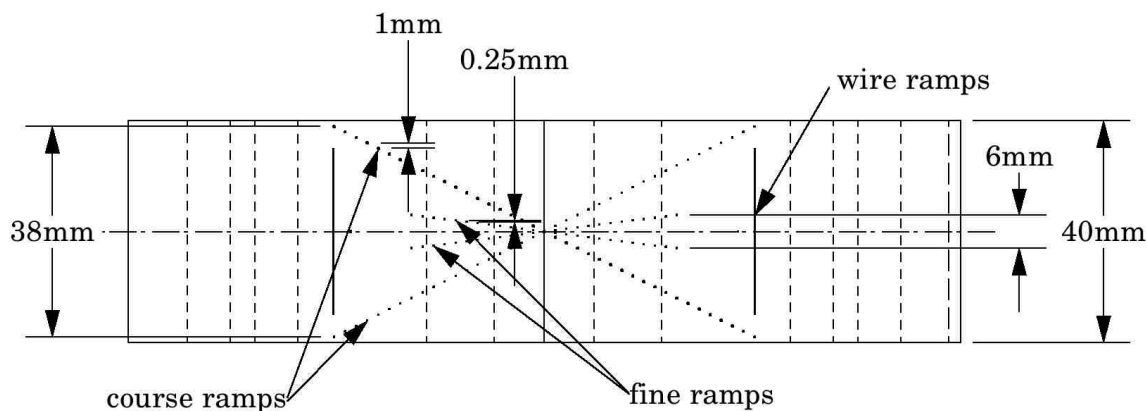
$$0.42(L1 - L2) = \text{scan incrementation}$$

This test can also be used to test table increment accuracy. Scan the section and increment the table 30mm in and out of the gantry and scan again. The ramp centers should be the same on both images.

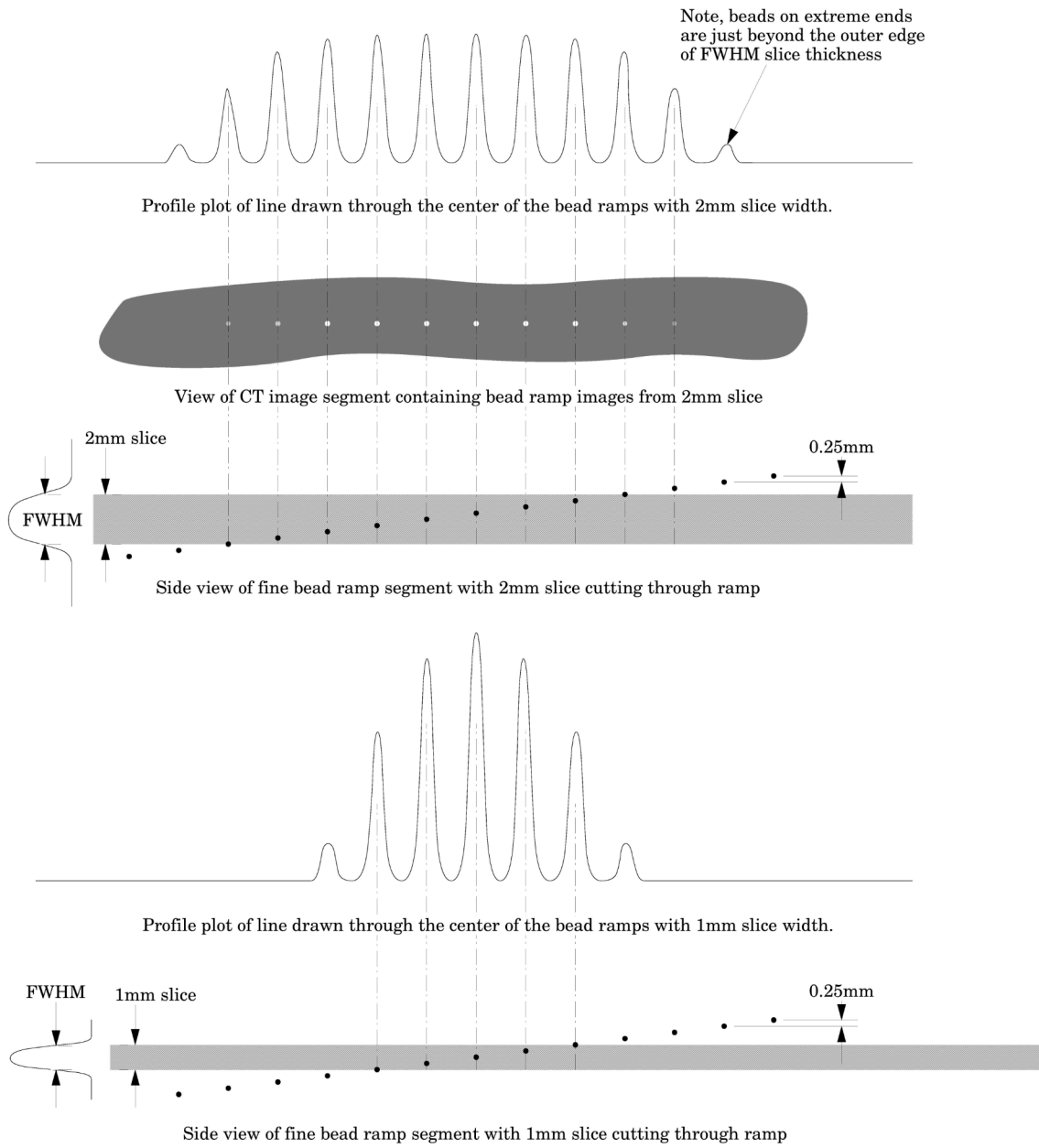
$$0.42(L1 - L2) = 0$$

### Slice Width Measurement with Bead Ramps

The CTP682 module contains 2 pairs of opposed bead ramps. The course ramp pair has 0.28mm diameter beads, spaced 1mm on center in the z direction. The fine ramp pair has 0.18mm diameter beads, spaced 0.25mm on center in the z direction. The 2 individual beads are 0.28mm and 0.18mm in diameter.

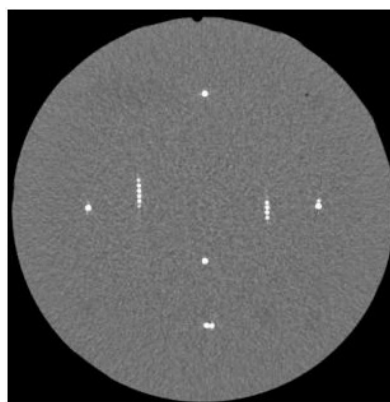


To demonstrate how the bead ramps are used, the illustration on the following page shows both a 1mm and 2mm slice going through a bead ramp. You may note that as the slice thickness increases, the peak CT value for the beads decrease. This is because as the slice thickness increases, the bead's effect on the CT number of the voxel decreases, due to volume averaging. Presuming the slice thicknesses are accurate and that the slice sensitivity profile has the same type of distribution, the peak signal over background in a 1mm slice should be approximately double that of the peak signal over the background in the 2mm slice.

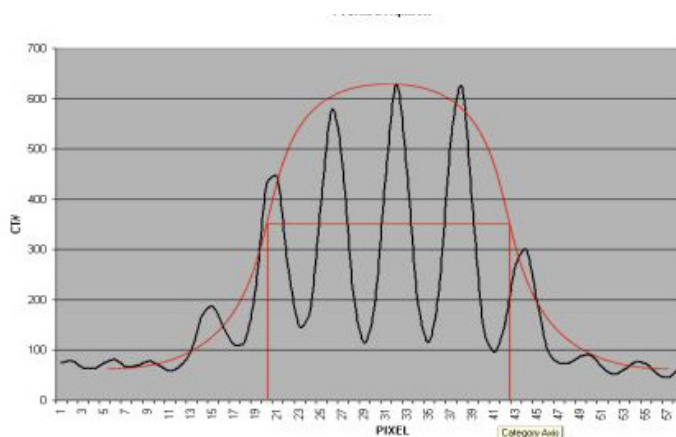


## Slice Thickness from a Profile of Bead Intensities

Please note in this example 0.25mm spaced slice ramps are used, rather than the 1mm spaced slice ramps. The methodology for both would be basically the same, however for thinner slices the use of the fine ramps improve measurement precision. Below we use a 1mm slice scan to illustrate the use of a profile made from a line running through the bead images on the scan.



Scan of CTP591 with 1mm slice width



Vertical Profile of a 1mm slice through the fine .025mm bead ramps after zooming or magnification

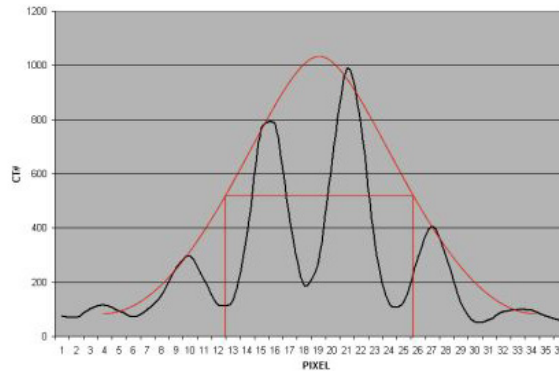
When we use a profile line through the beads, there will be peaks at each of the bead locations and these will be separated by 0.25mm from each other in the scanner's z direction. Thus for example, for the 1.0mm slice width we measure about four bead spacings at the Full Width at Half Maximum (FWHM). Multiplying the four bead spacings times the z-axis increment 0.25mm per bead yields a 1mm slice width.

Another method for counting beads would be to measure the maximum CT number of the beads. This can be done by adjusting the window width to 1 and raising the level until the beads disappear and noting the peak level. Next, do an ROI of the area adjacent to the ramp to get a number for the background. Keeping the window width at 1, raise the level to half between background and peak (half maximum) and count the beads.

We can make this somewhat more analytic by noting the following. If we hand-draw, or use a

mathematical “best fit” bell shaped curve (e.g. Gaussian) to the data points, you will notice that the peak CT number for the 1.0mm slice is about 650 H and the baseline is about 50, leaving a net value of about 600H between the peak value and the baseline. Thus,  $\frac{1}{2}$  the (net) maximum value is 300H + the baseline of about 50H so we draw a line across the 350H ordinate (Y) value and measure the length of the line that spans the two FWHM points at, in this case, 350H.

When measuring the FWHM of the curve it is important to realize that due to scaling and translation variables the scale of the FWHM length needs to be defined. This is done using the distance between the individual bead peaks in the profile whose absolute separation in the z axis is known (.25mm for fine ramps and 1mm for course ramps). For example for the fine ramps divide the FWHM by the distance between bead peaks and multiply by .25mm.



Vertical Profile of a 0.5mm slice through the fine .025mm bead ramps after zooming or magnification

Please note, the typical tolerance allowed is somewhere between 0.5mm and 10% depending on the vendor, and the slice thickness being measured.

### **Additional methods for estimating and measuring slice thicknesses with the bead ramps**

A slice sensitivity profile (SSP) of the bead(s) can be used to measure slice thickness (see the Bead point source section for additional information).

Sagittal and coronal slices through the beads can also be used to measure the axial slice width. In this case measure the z-axis length at the full width at half maximum of a bead image to establish the slice thickness. However, this technique is limited in precision z-axis of the voxels.

The volume averaging effect on the net peak CT number of the bead can be used to approximate additional slice thickness measurements after measuring one slice's thickness by using the following equation:

- w = slice width of additional slice thickness.
- npvm = net peak value of the bead in the measured slice width
- msw = slice width of the measured slice
- npva = net peak value of the bead in the additional slice width

$$w = (npvm / npva) * msw$$

Note: Net peak value = (CT# of the bead) - (CT# of the background)



## Patient Alignment System Check

The patient alignment lights can be checked for accuracy by using the white alignment markers on the phantom housing. Align the phantom as discussed in Initial phantom positioning and set the table position at 0. Please note that due to housing casting variations the alignment markers may be off by a couple millimeters from the center of the CTP482 module. For a quick check scan through the phantom at the 0 table position and check to see if you are in the center of the module.

For a more precise measurement, scan through the module using the thinnest available slice width. Scroll through the slices and select the slice with the highest CT value for the 3 alignment markers. Check the table position of the “selected slice”, if it is 0 your alignment lights are accurate, if the table position of the “selected slice” is different from the slice with a table position 0 then the alignment will be off by the distance from the 0 table position slice to the “selected slice”. The distance between the center of the two slices can also be measured by measuring the distance between lines running through the center of the ramp images in the two slices and multiplying this distance by  $.42, \tan(23^\circ)$ , the ramp scaling factor. See illustration on the next page.

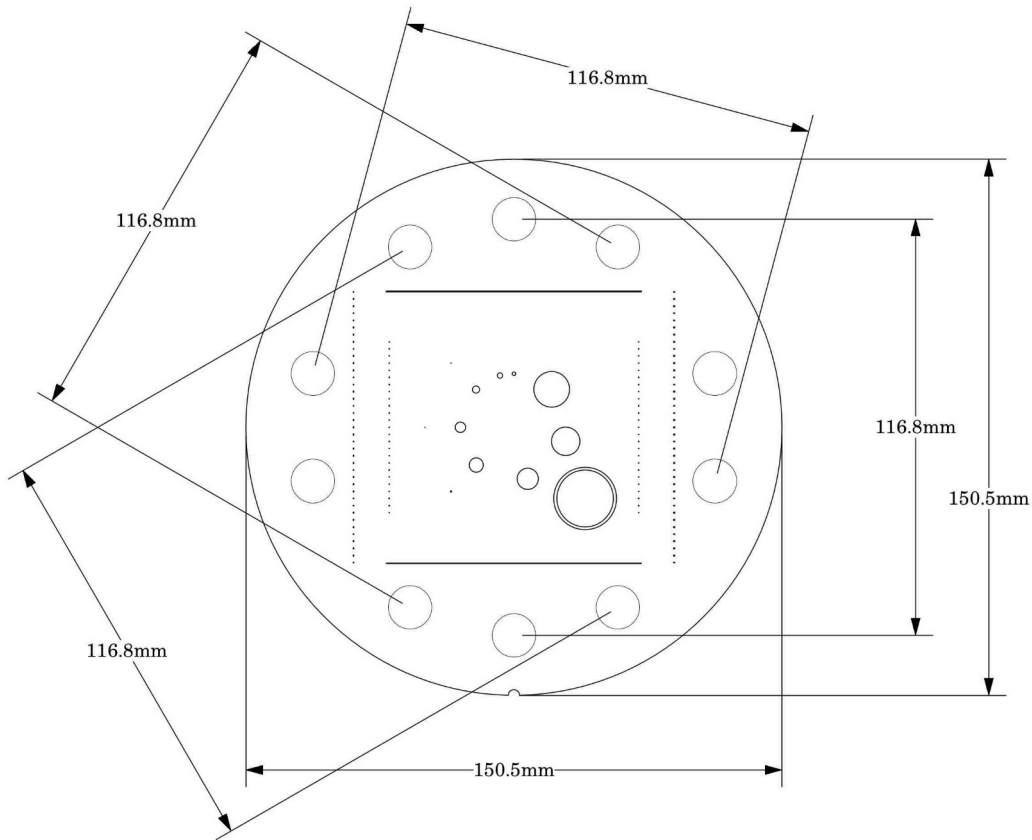
It is important to note that with some multi-slice, when an even number of slices is used, scanners the slice is not centered at zero. Instead the slice starts at zero. In this case the slice center will be  $1/2$  the slice width away from the zero position.

To evaluate x and y accuracy, measure from the center of the phantom to the center of the scan field by use of the grid function or knowledge of the central pixel location.

The accuracy of the localizer, pilot or scout view can be checked. To check this function perform a localization scan of the phantom. Align an axial scan at the crossing point of the wire ramps. Set this location of the table to 0. Scan through the CTP682 module using the thinnest available slices. Select the slice where the ramps are closest to the center. Compare this slice with the slice at the table position 0 as described above to measure the offset.

### Circular Symmetry of Display System

The circular phantom sections are used to test for circular symmetry of the CT image, including calibration of the CT display system. If an elliptical image is produced, the x-y balance of the image display system should be adjusted.

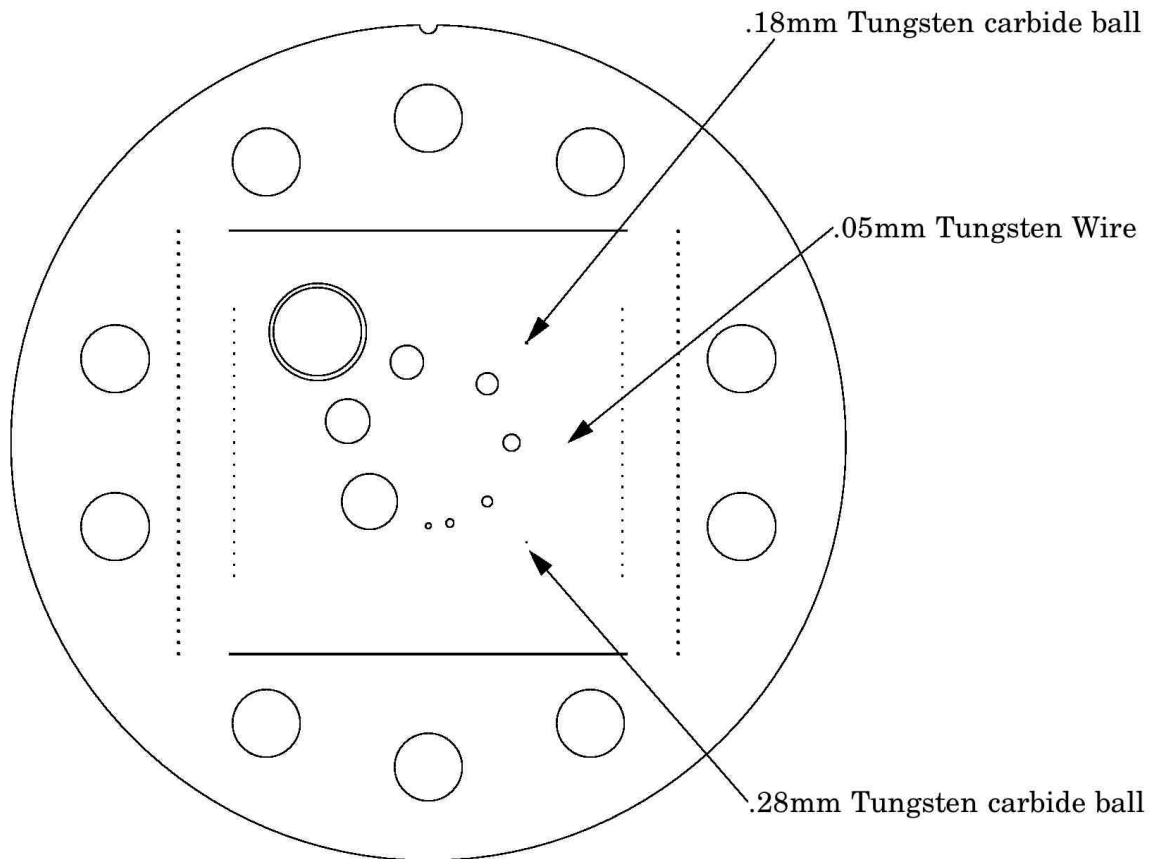


Measuring spatial linearity

### Spatial Linearity and Pixel Size Verification

The diameter of the module in the x and y-axes can be measured to verify the scanner's spatial linearity. This section has ten holes (with sensitometry targets). These 12.3mm diameter holes provide 5 diametrically opposed pairs measuring, center to center, 116.8mm apart. By measuring from center to center between the holes, or the diameter of the module, the spatial linearity of the CT scanner can be verified. Another use is to count the number of pixels between the hole centers. By knowing the distance and number of pixels, the pixel size can be verified.

### Bead or Wire Point Source for Determination of Point Spread Function and MTF

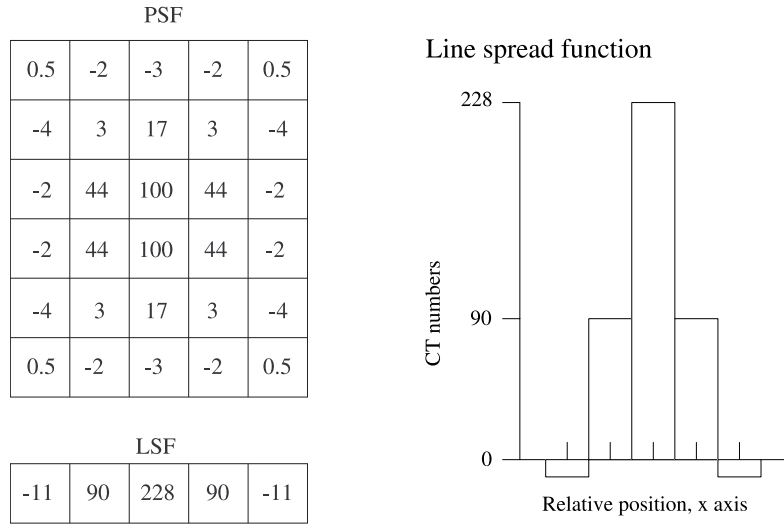


Use the bead or wire impulse source to estimate the point source response function of the CT system. Print out a digitized image of the area surrounding the impulse source. Use the numerical data to determine the two-dimensional array of the CT values arising from the impulse source.

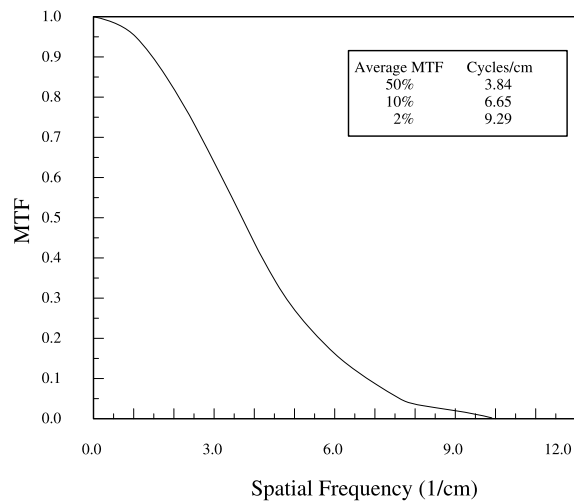
The FWHM of the point spread function is determined from the best-fit curve of the point spread function numerical data.

The average of several different arrays of impulse response functions is calculated to obtain the average point spread function of the system. These numerical values are used in conjunction with the Fourier Transform Program to provide an estimate of the two-dimensional spatial frequency response characteristics of the CT system (MTF). An illustration is on the next page.

The tungsten carbide bead has a diameter of 0.011" or 0.28mm. Because the bead is subpixel sized it is not usually necessary to compensate for it. However, some MTF programs are designed to compensate for its size.



The above illustration shows how by summing the columns (y-axis) of pixel numbers in the point spread function (PSF) the line spread function (LSF) for the x-axis is obtained. Likewise the (LSF) for the y-axis can be obtained by summing the rows (x-axis) data.



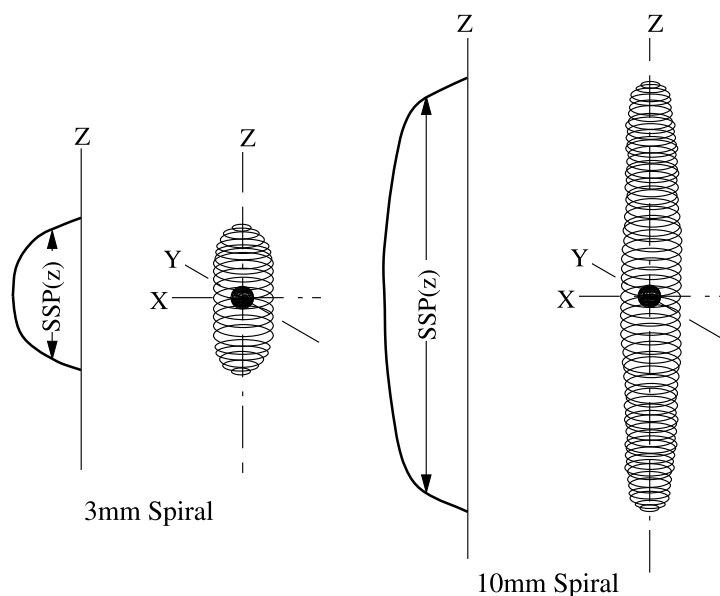
The MTF curve results from the Fourier Transform of the LSF data. Generally it is easiest to use automated software for this operation. Some CT scanners are supplied with software which can calculate the MTF from the Catphan® bead images.

### Use of Automated Scanner MTF Programs

Many manufacturers include automated MTF software in the standard scanner software packages. Because the bead is cast into an epoxy background which has a different density than water, the software must accept an input for the background CT number. The point size of 0.28mm for the large bead, 0.18mm for the small bead or 0.05mm for the wire must also be identified. While a sphere does produce a different density profile than a cross section of a wire or cylinder, both objects are so small that the actual difference is not usually significant in current CT scanners. The automated Smári analysis service automatically accounts for these variables in PSF and MTF calculations.

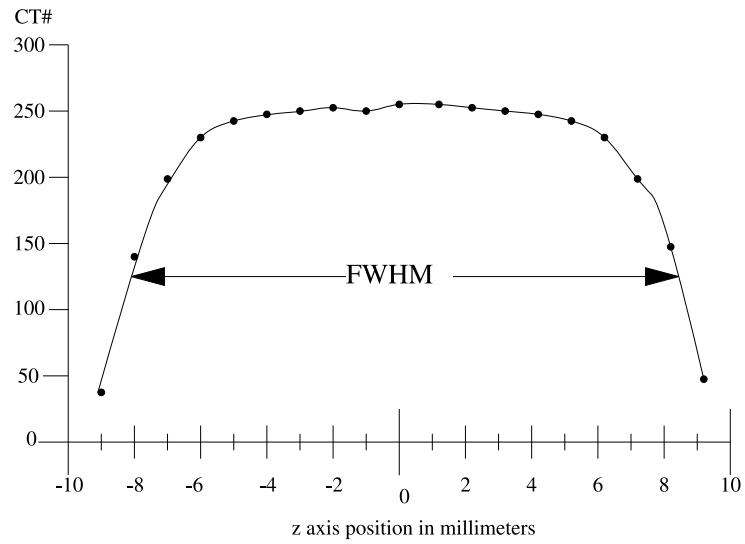
### Bead Point Source for Slice Sensitivity Profile

The bead in this module can be used to calculate the slice sensitivity profile (SSP).



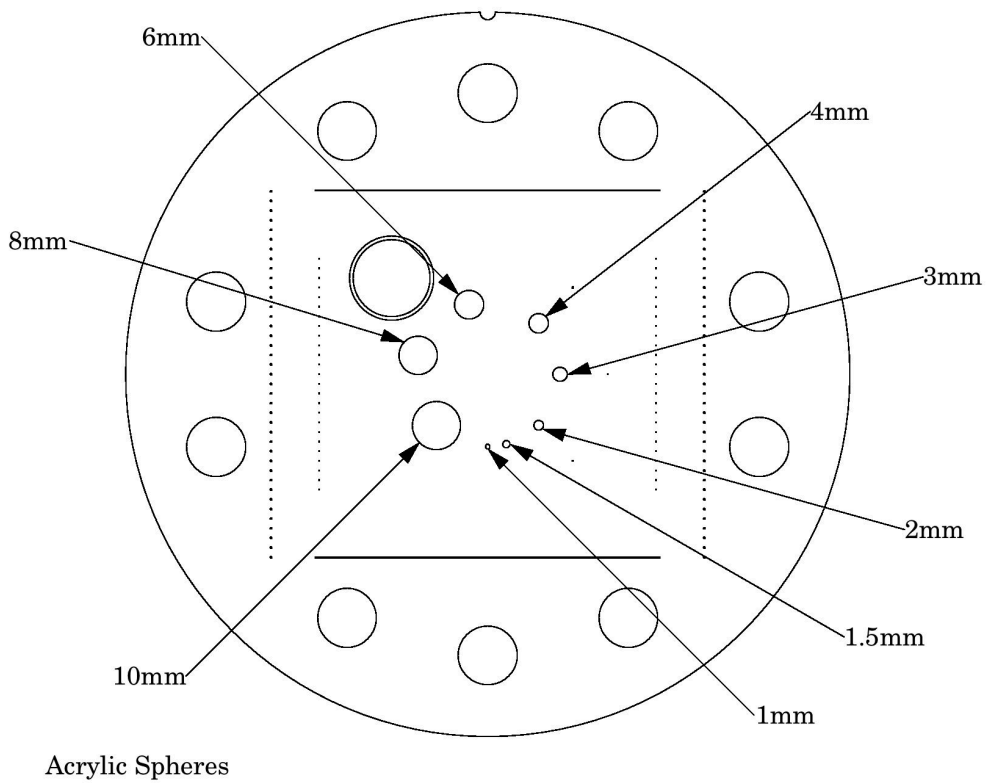
The above image illustrates how the bead will produce an ovoid object in a 3 dimensional reconstruction. The length of the object at the Full Width at Half Maximum signal indicates the SSP. This measurement can be easily obtained on some systems, by making a sagittal or coronal reconstruction through the bead. The bead image in these reconstructions will appear as a small line. By setting the FWHM (use the same technique described in the **Scan slice geometry** section) measuring the z-axis length of the bead image to obtain the SSP.

If the scanner does not have the ability to measure z-axis lengths in the sagittal or coronal planes, a SSP can be made by incrementing or spiraling the slice through the bead and reconstructing images in positive and negative table directions from the bead (using the smallest available increments) and plotting the peak CT number of the bead image in each slice. The FWHM measurement can then be made from the plotted CT values of the bead as a function of z-axis table position.



### Spherical acrylic contrast targets

The CTP682 module has 8 acrylic spheres located in a 30mm diameter circular pattern. These spheres are used to evaluate the scanner's ability to image volume averaged spheres. The sphere diameters are 1, 1.5, 2, 3, 4, 6, 8, and 10mm.



## CT or Hounsfield Numbers by David Goodenough, Ph.D.

Users of CT systems are often surprised when the CT number of a given tissue or substance is different from what they expect from previous experience. These differences do not usually indicate problems of a given CT scanner, but more likely arise from the fact that CT numbers are not universal. They vary depending on the particular energy, filtration, object size and calibration schemes used in a given scanner. One of the problems is that we are all taught that the CT number is given by the equation:

$$CT\# = k(\mu - \mu_w)/\mu_w$$

where  $k$  is the weighting constant (1000 is for Hounsfield Scale),  $\mu$  is the linear attenuation coefficient of the substance of interest, and  $\mu_w$  is the linear attenuation coefficient of water. Close review of the physics reveals that although the above equation is true to first order, it is not totally correct for a practical CT scanner. In practice,  $\mu$  and  $\mu_w$  are functions of energy, typical x-ray spectra are not monoenergetic but polychromatic, and a given spectrum emitted by the tube is “hardened” as it is transmitted (passes) through filter(s) and the object, finally reaching the detector. More accurately,  $\mu = \mu(E)$ , a function of energy. Therefore:

$$CT\#(E) = k(\mu(E) - \mu_w(E))/\mu_w(E)$$

Because the spectrum is polychromatic we can at best assign some “effective energy”  $\hat{E}$  to the beam (typically some 50% to 60% of the peak kV or kVp). Additionally, the CT detector will have some energy dependence, and the scatter contribution (dependent on beam width and scanned object size, shape, and composition) may further complicate matters. Although the CT scanner has a built in calibration scheme that tries to correct for beam hardening and other factors, this is based on models and calibration phantoms that are usually round and uniformly filled with water, and will not generally match the body “habitus” (size, shape, etc.).

The situation is really so complicated that it is remarkable that tissue CT numbers are in some first order ways “portable”!

In light of the above we can examine a parameter of CT performance, the “linearity scale”, as required by the FDA for CT manufacturer’s performance specifications.

The linearity scale is the best fit relationship between the CT numbers and the corresponding  $\mu$  values at the effective energy  $\hat{E}$  of the x-ray beam.

The effective energy  $\hat{E}$  is determined by minimizing the residuals in a best-fit straight line relationship between CT numbers and the corresponding  $\mu$  values.

In review, we will encounter considerable inter and intra scanner CT number variability. CT numbers can easily vary by 10 or more based on kVp, slice thickness, and object size, shape, and composition. There is some possibility of the use of iterative techniques and/or dual energy approaches that might lessen these effects, but certainly CT numbers are not strictly portable and vary according to the factors listed above.

More complete scientific references are contained in the bibliography. In particular, references 2, 13, 14, and 20 are recommended for those with greater interest in the topic.

### Sensitometry (CT number linearity)

The CTP682 module has sensitometry targets made from Teflon®, Bone 50%, Delrin®, Bone 20%, acrylic, Polystyrene and low density polyethylene (LDPE), polymethylpentene (PMP), Lung foam #7112 and air. The module is also equipped with a small removable vial which can be filled with water or other material and inserted into the CTP682 module.

These targets range from approximately +1000 H to -1000 H. A table with the linear attenuation coefficient  $\mu$  [units  $\text{cm}^{-1}$ ] can be downloaded from our web site.

The monitoring of sensitometry target values over time can provide valuable information, indicating changes in scanner performance. Note, values can change depending on local temperature and pressure.

#### Nominal material formulation and specific gravity

<u>Material</u>	<u>Formula</u>	<u><math>Z_{\text{eff}}^1</math></u>	<u>Specific Gravity<sup>2</sup></u>	<u>HU range<sup>3</sup></u>
Air	.78N, .21O, .01Ar	8.00	0.00	-1046 : -986
Lung #7112	[C <sub>38</sub> H <sub>38</sub> NgO <sub>15</sub> ]	6.64	0.19	-925 : -810
PMP	[C <sub>6</sub> H <sub>12</sub> (CH <sub>2</sub> )]	5.44	0.83	-220 : -172
LDPE	[C <sub>2</sub> H <sub>4</sub> ]	5.44	0.92	-121 : -87
Water	[H <sub>2</sub> O]	7.42	1.00	-7 : 7
Polystyrene	[C <sub>8</sub> H <sub>8</sub> ]	5.70	1.03	-65 : -29
Acrylic	[C <sub>5</sub> H <sub>8</sub> O <sub>2</sub> ]	6.47	1.18	92 : 137
Bone 20%	.51C, .06Ca, .06H, .06N, .30O, .03P	9.09	1.14	211 : 263
Delrin®	Proprietary	6.95	1.42	344 : 387
Bone 50%	.35C, .14Ca, .04H, .06N, .34O, .06P	11.46	1.40	667 : 783
Teflon®	[CF <sub>2</sub> ]	8.43	2.16	941 : 1060

#### Electron density and relative electron density

<u>Material</u>	<u>Electron Density (<math>10^{23}</math> e/g)</u>	<u>Electron Density (<math>10^{23}</math> e/cm<sup>3</sup>)</u>	<u>Relative Electron Density<sup>4</sup></u>
Air	3.002	0.004	0.001
Lung #7112	3.144	0.588	0.176
PMP <sup>5</sup>	3.435	2.851	0.853
LDPE <sup>6</sup>	3.435	3.160	0.945
Water	3.343	3.343	1.000
Polystyrene	3.238	3.335	0.998
Acrylic	3.248	3.833	1.147
Bone 20%	3.178	3.623	1.084
Delrin®	3.209	4.557	1.363
Bone 50%	3.134	4.387	1.312
Teflon®	2.890	6.243	1.868

<sup>1</sup>  $Z_{\text{eff}}$ , the effective atomic number, is calculated using a power law approximation.

<sup>2</sup> For standard material sensitometry inserts Phantom Laboratory purchases a multiple year supply of material from a single batch. Samples of the purchased material are then measured to determine the actual specific gravity. The specific gravity of air is taken to be .0013 at standard temperature and pressure. For custom cast materials the specific gravity of each cast batch is noted and supplied with the phantom. The lung #7112 is a



foam, and while it is purchased in large batches it varies through out the batch. For this reason the lung numbers may have a greater variation.

<sup>3</sup>These are maximum and minimum measured values from a sample of 94 scans using different scanners and protocols. HU can vary dramatically between scanners and imaging protocols and numbers outside of this range are not unusual.

<sup>4</sup> Relative Electron Density is the electron density of the material in  $e/cm^3$  divided by the electron density of water ( $H_2O$ ) in  $e/cm^3$ .

<sup>5</sup> Polymethylpentene

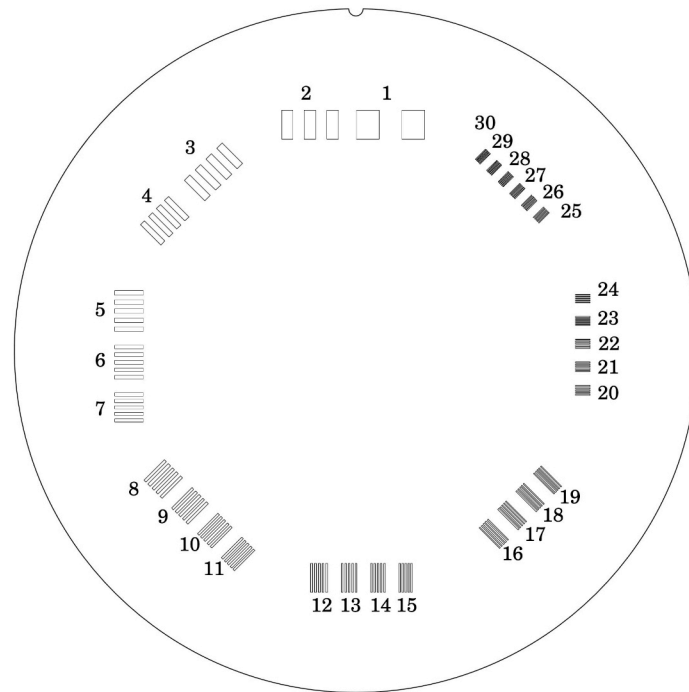
<sup>6</sup> Low Density Polyethylene

An excel file with the mas attenuation coefficients for the sensitometry materials can be downloaded from our web site.

### **Filling the water vial**

To fill the water vial, pull the vial out of the phantom and remove the lid. The use of distilled water eliminates possible variables due to tap water purity. Submerge the container and lid under water and position so all air escapes then tighten the lid onto the vial preventing air from entering the vial. Dry off the vial and insert it back into the CTP682 module. Check that no air bubbles remain in the vial and allow the vial to return to normal room temperature.

### CTP714 High Resolution Module with 1 to 30 line pair/cm Gauges



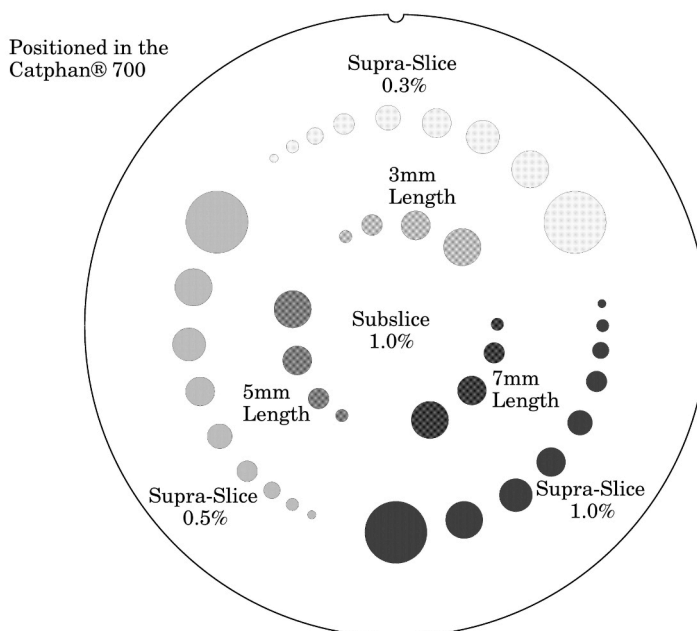
The 30 line pair/cm gauge has resolution tests for visual evaluation of high resolution ranging from 1 through 30 line pair/cm. The gauge accuracy is  $\pm 0.5$  line pair at the 30 line pair test and even better at lower line pair tests.

The gauge is cut from 2mm thick aluminum sheet and cast into clear urethane. Depending on the choice of slice thickness, the contrast levels will vary due to volume averaging. By use of the rotation mount, the phantom can be rotated so gauges are either aligned with one of the scanner axes or set at 45° angles to the axis.

Line Pair/cm	Gap Size	Line Pair/cm	Gap Size	Line Pair/cm	Gap Size
1	0.500 cm	11	0.045 cm	21	0.024 cm
2	0.250 cm	12	0.042 cm	22	0.023 cm
3	0.167 cm	13	0.038 cm	23	0.022 cm
4	0.125 cm	14	0.036 cm	24	0.021 cm
5	0.100 cm	15	0.033 cm	25	0.020 cm
6	0.083 cm	16	0.031 cm	26	0.019 cm
7	0.071 cm	17	0.029 cm	27	0.0185 cm
8	0.063 cm	18	0.028 cm	28	0.0178 cm
9	0.056 cm	19	0.026 cm	29	0.0172 cm
10	0.050 cm	20	0.025 cm	30	0.0167 cm

A line pair contains one gap and one aluminum element. For example 1 line pair/cm gauges include .5cm gaps and .5cm aluminum elements.

### CTP515 Low Contrast Module with Supra-slice and Subslice Contrast Targets



The low contrast targets have the following diameters and contrasts:

Supra-slice target diameters  
(outer circle of targets)

2.0mm  
3.0mm  
4.0mm  
5.0mm  
6.0mm  
7.0mm  
8.0mm  
9.0mm  
15.0mm

Subslice target diameters  
(inner circle of targets)

3.0mm  
5.0mm  
7.0mm  
9.0mm

Nominal target contrast levels ( $\pm 0.05\%$ )

.3%  
.5%  
1.0%

Since the target contrasts are nominal, the actual target contrasts need to be determined before testing specific contrast performance specifications. The actual contrast levels are measured by making region of interest measurements over the larger target, and in the local background area. To determine actual contrast levels, average the measurements made from several scans.

It is important to measure the background area adjacent to the measured target because “cupping” and “capping” effects cause variation of CT numbers from one scan region to another. Position the region of interest to avoid the target edges. The region of interest should be at least 4 x 4 pixels in

diameter. Because low contrast measurements are “noisy”, it is advisable to calculate the average of the multiple measurements made from several scans. Carefully monitor the mAs setting and the presence of any dose-modulation and or dose reducing methods being used, because the photon flux will improve with increased x-ray exposure. The size of the targets visualized under various noise levels can be used to estimate information on contrast detail curves.

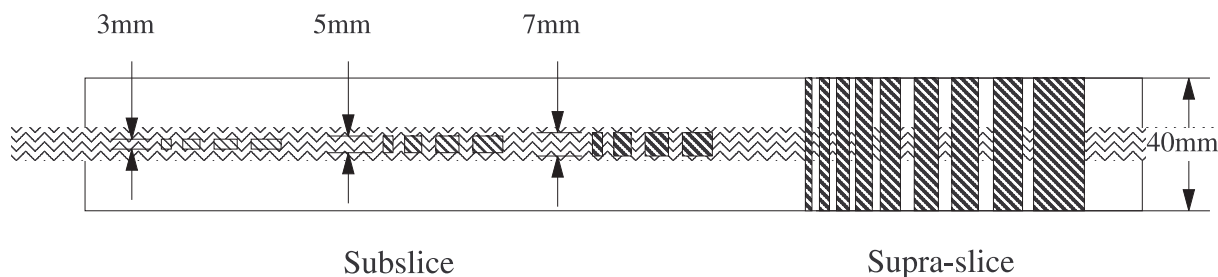
All of the targets in each contrast group are cast from a single mix to assure that the contrast levels will be the same for all targets.

The equation below can be used in conjunction with other published models of target detection in CT, to convert the measured contrasts and diameters to other estimated specified contrasts and diameters.

(Measured Contrast) \* (smallest diameter discernible) @ Constant

example: 5mm diameter @ 0.3% @ 3mm diameter @ 0.5% @ 1.5

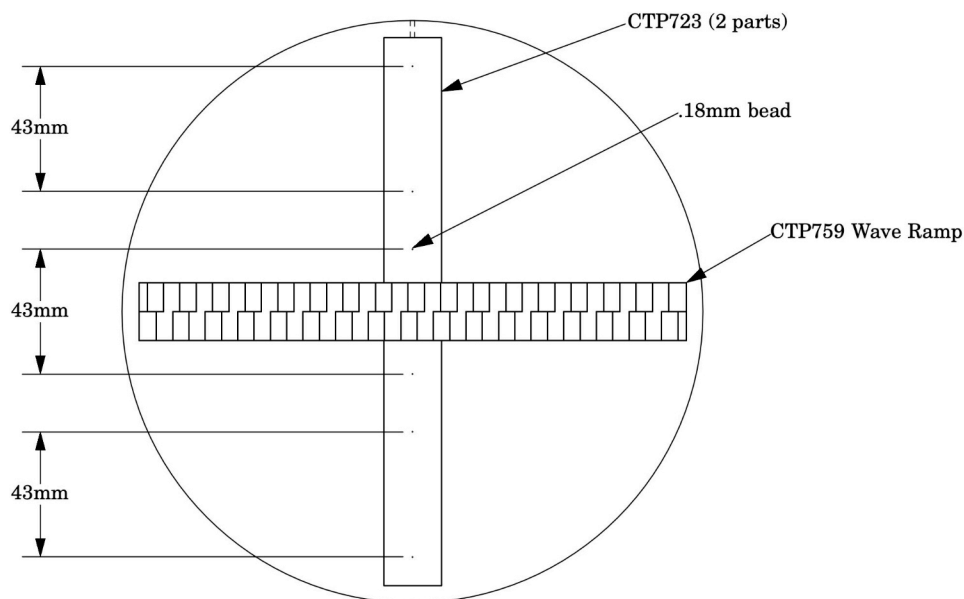
Along with the supra-slice (targets with z-axis dimension longer than most maximum slice width) the CTP515 low contrast module includes subslice targets (targets with z-axis length smaller than some of the usual slice width). The subslice targets are arranged in the inner circle of tests in the module.



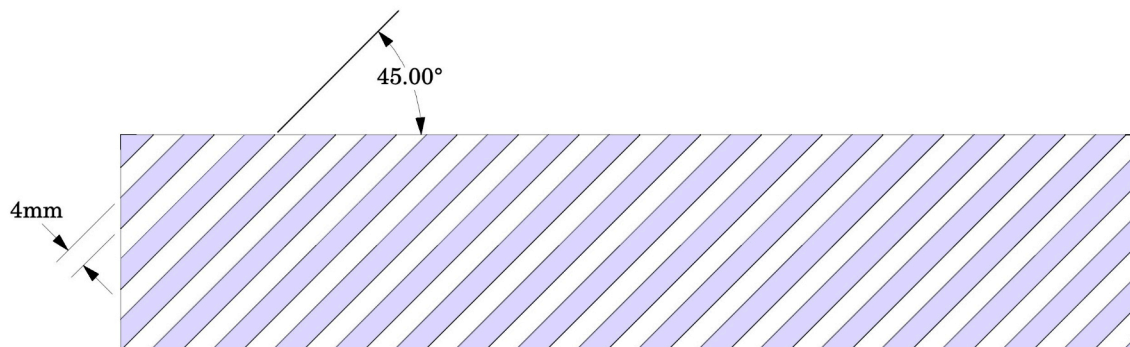
The subslice targets are cast from the same mix as the 1.0% supra-slice targets. Because they are from the same mix, in the evaluation of the actual subslice target contrast the supra-slice targets can be used to establish contrast values. The subslice targets have z-axis lengths of 3, 5, and 7mm and diameters of 3, 5, 7, and 9mm.

The evaluation of subslice target readability is helpful in understanding the scanner’s different performance with varying slice width and axial (sequential) scanning, and spiral imaging settings and how the settings will affect the ability to visualize small objects with low contrasts from their background.

## Wave Ramp and Bead Modules



The wave ramp is designed to look at the slice geometry across the phantom as impacted by both in-plane resolution and z-axis (slice thickness) resolution. This is achieved by offering a periodic pattern that is angled through the z axis at a given ramp angle. By analyzing a profile through the two ramps, information on the 3D voxel resolution is revealed. In addition, six point sources are also offered in the phantom to provide simultaneous information on the in-plane psf, and resulting MTF.

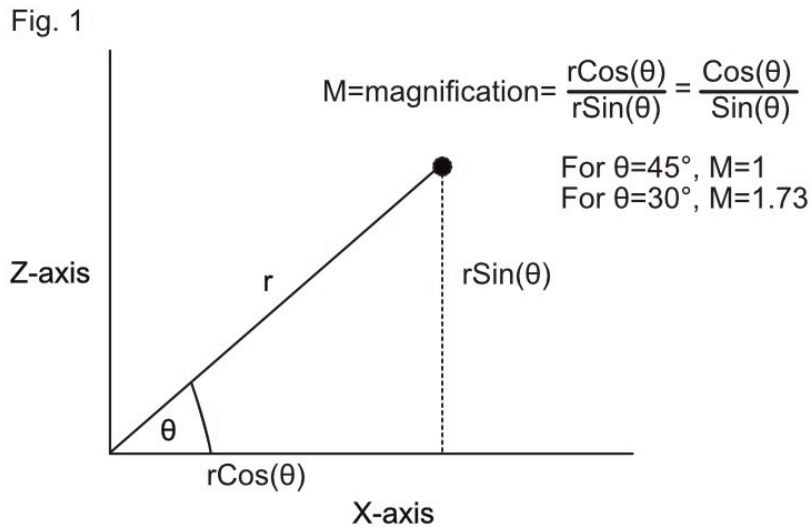


There are two opposing ramps manufactured from aluminum. The 4mm thick aluminum ramps are spaced between 4mm thick urethane material. Thin slice scans through the Wave Ramp Insert create oscillating patterns. The Smári Analysis Service will use the FFT function from these oscillating patterns to calculate the harmonic amplitudes of the critical frequencies. These frequencies reflect the voxel resolution.

### Background on the Wave Insert By David J. Goodenough, Ph.D.

**Challenge** – How to measure the 3-D (x,y,z) resolution properties in a single 2-D (x,y) CT scan?

**Solution** – By use of the Wave angled ramp pattern, we trigonometrically “project” z-axis effects into the x-y plane



If we want to study the z-axis slice sensitivity profile (SSP) in the z-direction,  $SSP(z)$ , or its corresponding  $MTF_z(v)$ , we can use the fact that when we combine point spread functions (psf),  $psf(1)$  and  $psf(2)$ , the net effect for linear, isoplanatic systems is a convolution<sup>⊗</sup> :

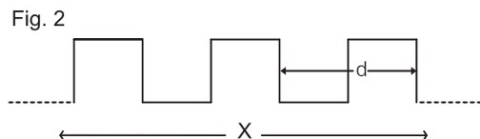
$$psf(1,2) = psf(1) \otimes psf(2)$$

and the corresponding MTF (1,2) combination is a multiplication:

$$MTF(1,2) = MTF(1) \times MTF(2)$$

For the wave ramp square wave pattern: For a particular spacing pattern of the bars where the pattern repeats at “d” spacing:

In real space (x or y)



The Fourier Transform (FT) of the wave is the series of harmonic amplitudes (A) as a function of spatial frequency  $A(v)$ , corresponding to the inverse spacing of the fundamental frequency. Wave  $v = \frac{1}{d}$  at  $1v, 3v, 5v \dots$ , at multiples of the fundamental frequency.

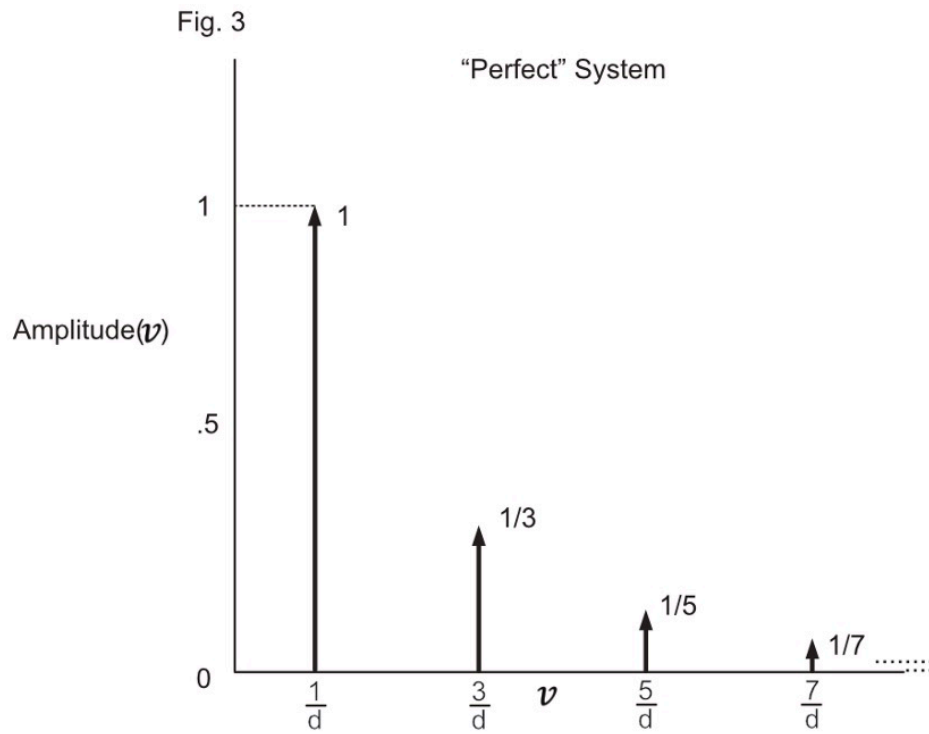


Figure 3 would be the transform of the wave from a "perfect" image system with no degradation due to x, y or z loss of spatial resolution or MTF in any axis.

Fig. 4

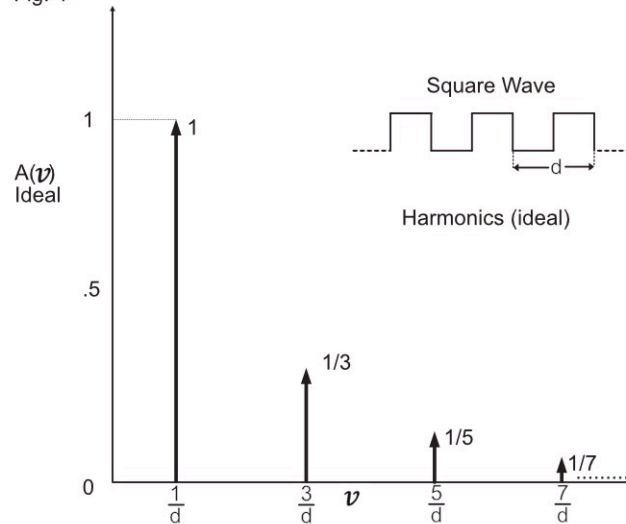
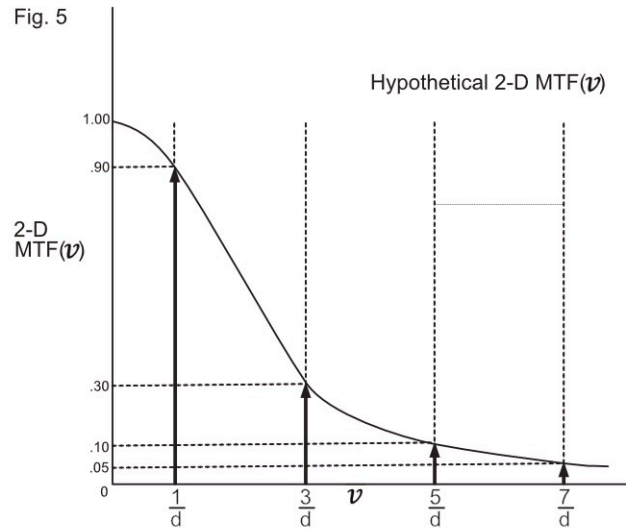


Fig. 5

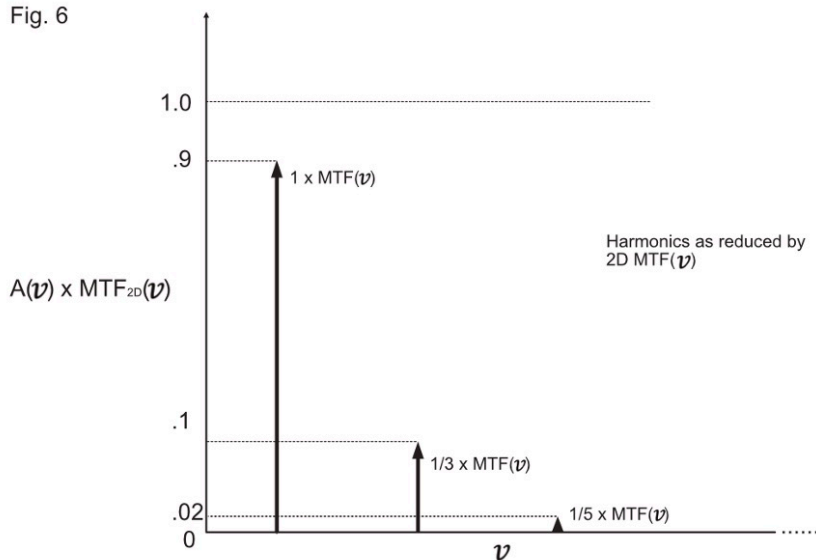


As shown in Figs. 4, 5 and 6 the actual amplitudes  $A(v)$  that would be measured from the CT scan of the Wave would be reduced proportionally by the 2D  $MTF(v)$ , and additionally by the  $MTF_z(v)$ , the transform of the  $SSP(z)$ , as discussed in the following figures.

Let us presume that the 2D  $MTF(v)$  from the bead transform would have the following amplitudes at the first 4 harmonics: 1<sup>st</sup>  $\rightarrow$  0.9, 2<sup>nd</sup>  $\rightarrow$  0.3, 3<sup>rd</sup>  $\rightarrow$  0.1, 4<sup>th</sup>  $\rightarrow$  0.05. These 2D MTF values are shown in Figure 5, and then further shown to reduce the harmonic amplitudes as shown in Figure 6.



Fig. 6



### Effects of Slice Thickness and SSP(z)

In reality the slice has some finite thickness (typically 0.5mm – 5mm) and so the SSP (z) will have a Fourier Transform  $MTF_z(v) < 1$ , much like the 2D MTF, further reducing the amplitude  $A(v)$ .

This is where the wave angle can help improve the measurement of the  $MTF(v)$ . By using a z-axis (slice width direction) magnification of 1.73 to take account of the angle of the ramps (in this case  $30^\circ$ ), we essentially SCALE the frequency axis  $v$  OR see the magnitude of  $MTF_z(v)$  moved to lower spatial frequencies to increase sensitivity. The correction for scaling is made in the software analysis package, or can be calculated manually. Let us presume a typical  $MTF_z(v)$  for the slice (z) direction as follows:

Fig. 7

e.g.

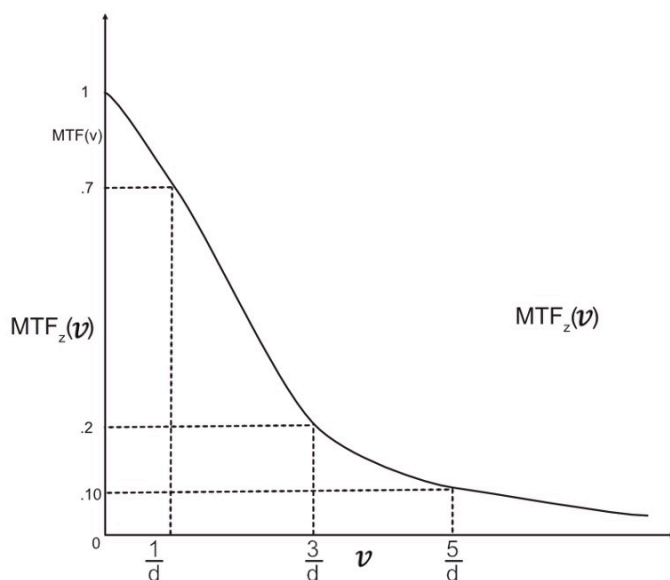
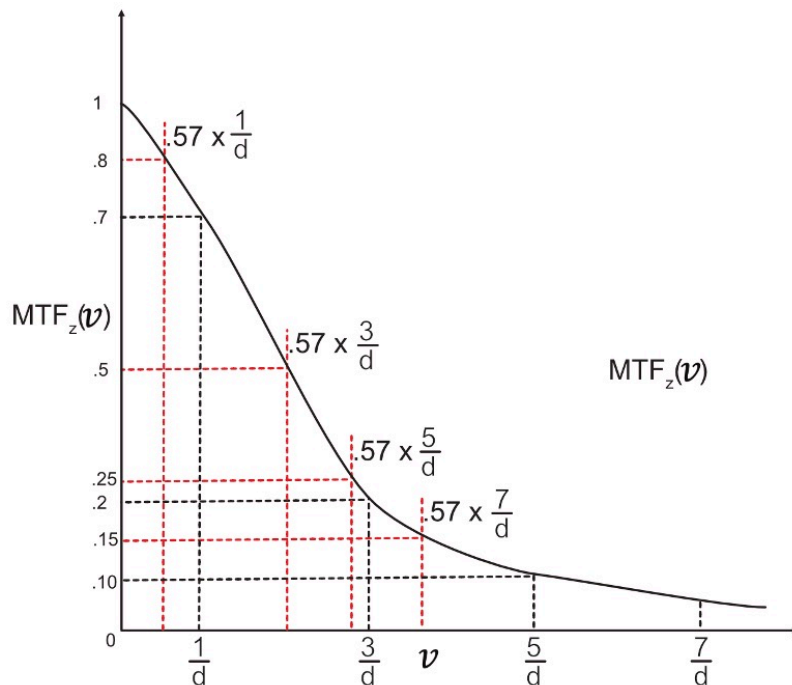


Fig. 8

e.g.



This “scaled”  $MTF_z(v)$  will increase the measured harmonic amplitudes to 0.8, 0.5, 0.25, 0.15, etc., because the scaled harmonic frequencies are reduced by a factor of 0.57 compared to the unscaled values of 0.7, 0.2, 0.1, etc.

Fig. 9

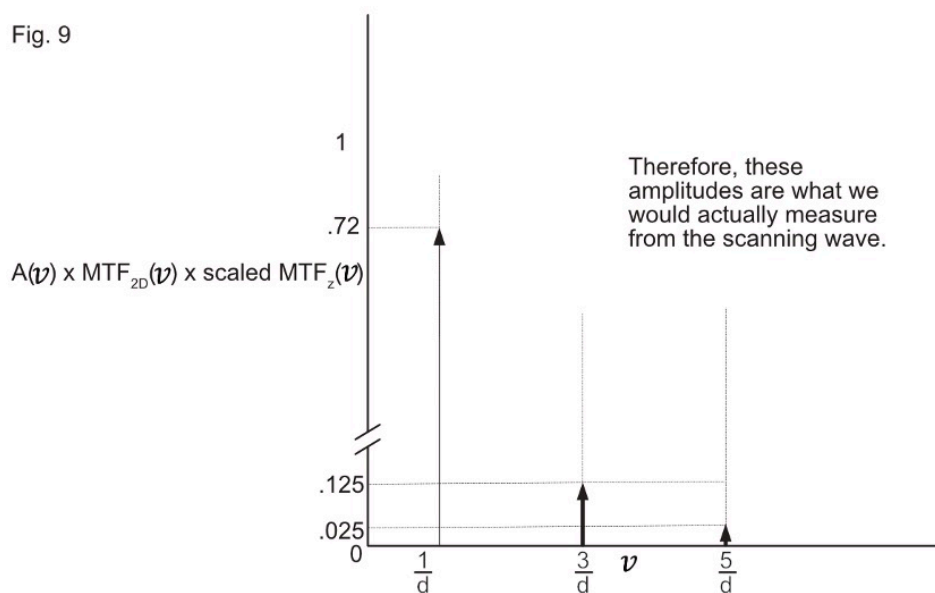


Table 1

<u>At Harmonics</u>	
e.g.	$A(v) \rightarrow 1, \frac{1}{3}, \frac{1}{5}, \frac{1}{7}, \dots$
	$MTF_{2D}(v) \rightarrow .9, .3, .1, .05, \dots$ <i>at harmonics</i>
and,	$scaled\ MTF_z(v) \rightarrow .8, .5, .25, .15, \dots$ <i>at harmonics</i>
	$MTF_{2D}(v) \times scaled\ MTF_z(v) \rightarrow .72, .15, .025, 0, \dots$
	<i>That is, measured wave harmonics</i> $A(v) \rightarrow .72, .05, .005, \dots$

Returning to the main point of the influence of wave ramp angle:

We measure wave harmonic amplitudes as a function of spatial frequency,  $A(v)$ , and note that these amplitudes are

“reduced” from the theoretical values of  $1, \frac{1}{3}, \frac{1}{5}, \frac{1}{7}, \dots$  etc. by the combined effects of the 2D MTF (which we can

measure from the psf bead), and the scaled  $MTF_z(v)$ .

$$A(v)_{measured} = A(v)_{theoretical} \times MTF_{2D}(v) \times scaled\ MTF_z(v)$$

The actual  $MTF_z(v)$  of the SSP as shown in Table 1 are obtained by:

$$\frac{MTF_z(v)}{\text{Slice Thickness}} \Rightarrow FT\ of\ SSP(z)$$

$$scaled\ MTF_z(v) = \frac{A(v)_{measured}}{A(v)_{theoretical}} \bigg/ MTF(v)_{2D\ measured}$$

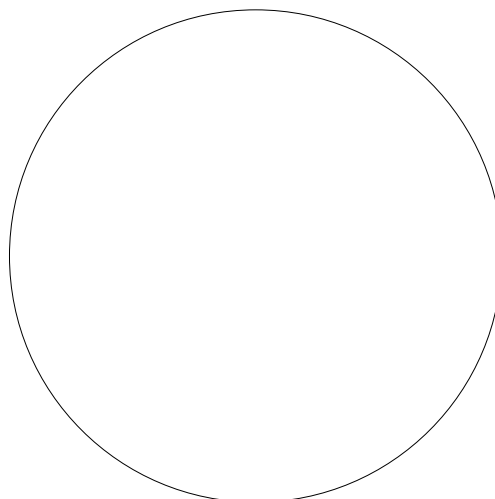
*noting, all are a function of (v)*

Where  $A(v)$  are amplitude data points at the distinct harmonic frequencies  $\frac{1}{d}, \frac{3}{d}, \frac{5}{d}$ , etc.

We know the effect of the in-plane (2D) and scaled z-axis MTF's was to reduce the harmonic amplitudes and combined MTF by these combined MTF factors, so the  $MTF_z(v)$  would have been = 0.8, 0.5, 0.25, 0.15, ... (at 0.577 x the harmonic frequency points).

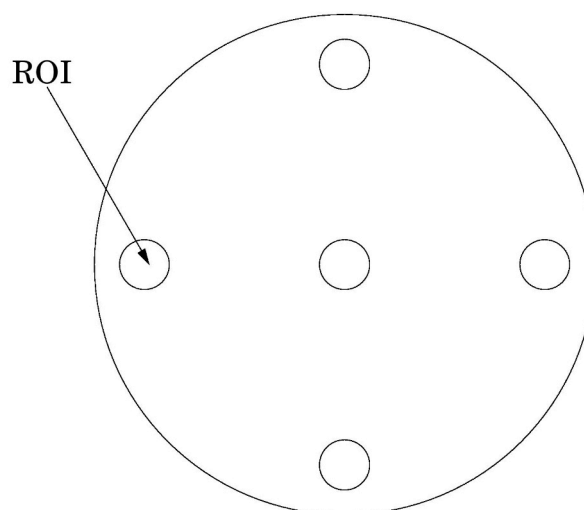
**Caution:** As discussed in these notes, the wave ramp angle must be checked against the latest production version, and software and/or manual calculations must take into account the actual ramp angle.

## CTP712 Image Uniformity Module



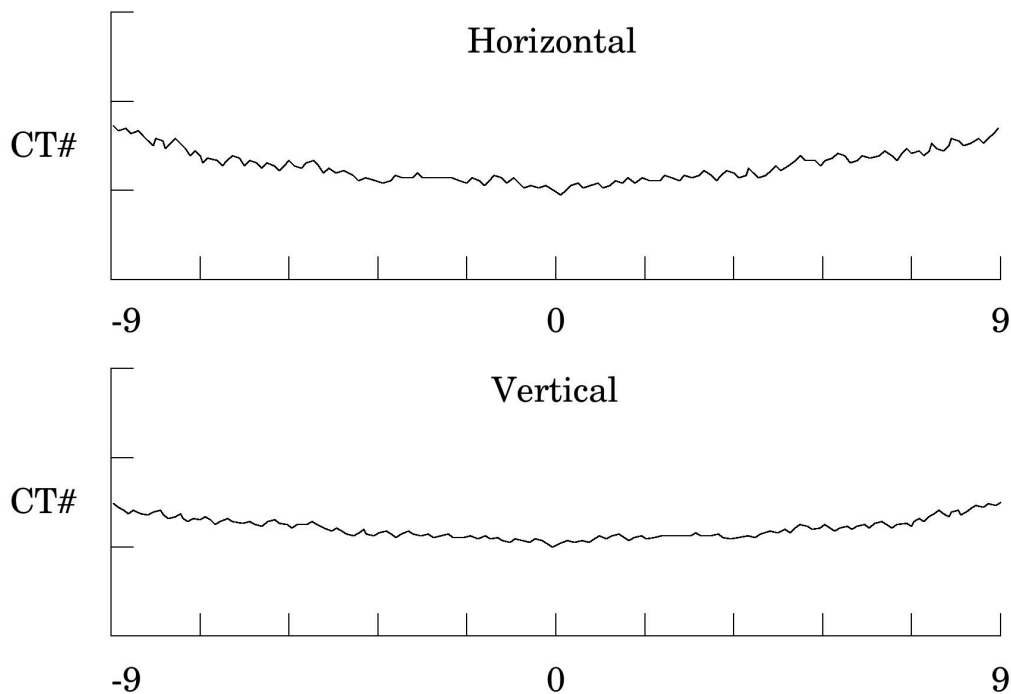
The image uniformity module is cast from a uniform material. The material's CT number is designed to be within 2% (20H) of water's density at standard temperature and standard scanning protocols. The typically recorded CT numbers range from 5H to 18H. This module is used for measurements of spatial uniformity, mean CT number and noise value.

The precision of a CT system is evaluated by the measurement of the mean value and the corresponding standard deviations in CT numbers within a region of interest (ROI). These measurements are taken from different locations within the image uniformity module. The deviation from the central mean ROI and or the mean value over the module as a whole (excluding the region near the boundary of the object) is measured.



The mean CT number and standard deviation of a large number of points, (say 1000 for example) in a given ROI of the scan, is determined for central and peripheral locations within the scan image for each type of scanning protocol.

Inspect the data for changes from previous scans and for correlation between neighboring slices.



Measure spatial uniformity by scanning the uniformity section. Observe the trends above and below the central mean value of a CT number profile for one or several rows or columns of pixels as shown above.

Select a profile which runs from one side of the uniformity module to the opposite side. Due to scanner boundary effects, typical profiles start one ROI, or about 2cm, from the edge of the test module.

Integral uniformity may be measured by determining the minimum and maximum CT values along the profile and by using the following equation :

$$\text{Integral Non-Uniformity} = \text{CT}_{\text{max}} - \text{CT}_{\text{min}}$$

$$\text{CT}_{\text{max}} + \text{CT}_{\text{min}}$$

$$\text{Integral Uniformity} = 1 - \left( \frac{\text{Integral Non-Uniformity}}{\text{CT}_{\text{max}} + \text{CT}_{\text{min}}} \right)$$

The phenomenon of “cupping” or “capping” of the CT number may indicate the need for recalibration.

## Smári Analysis Service

# Smári

For fast and accurate CT analysis, your new Catphan® purchase includes 2 years of the Smári analysis service

To register for the service, go to the Smári page at our website: [phantomlab.com](http://phantomlab.com)

You will need your phantom serial number to register, which is located on the phantom mount.



Once we receive your information, Phantom Laboratory support will contact you and set up your account.

Smári provides cloud-based automated analysis of your Catphan® phantom and tools such as longitudinal history and user specified alerts.

Test reports include:

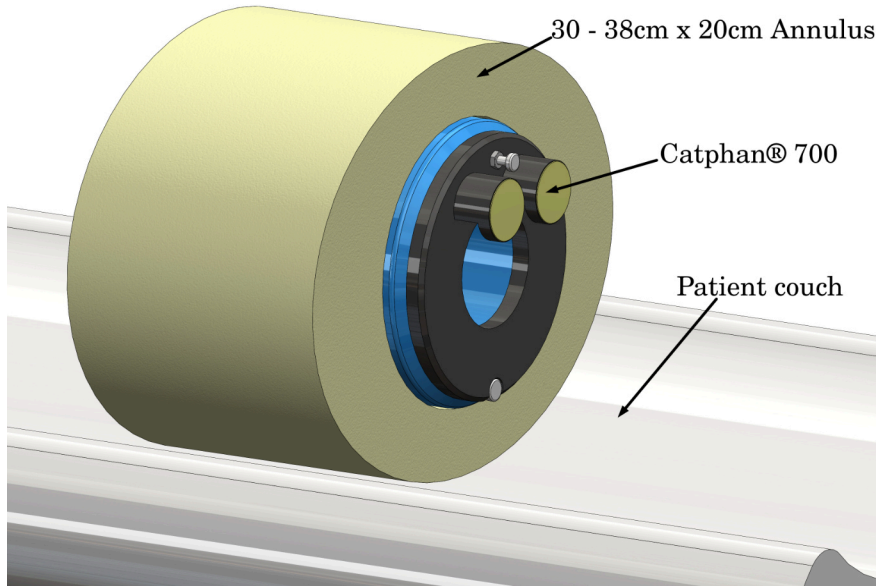
- Spatial resolution (modulation transfer function)
- Noise and image uniformity
- Slice width and pixel size
- Sensitometry
- Contrast detectability

## Optional Phantom Annuli

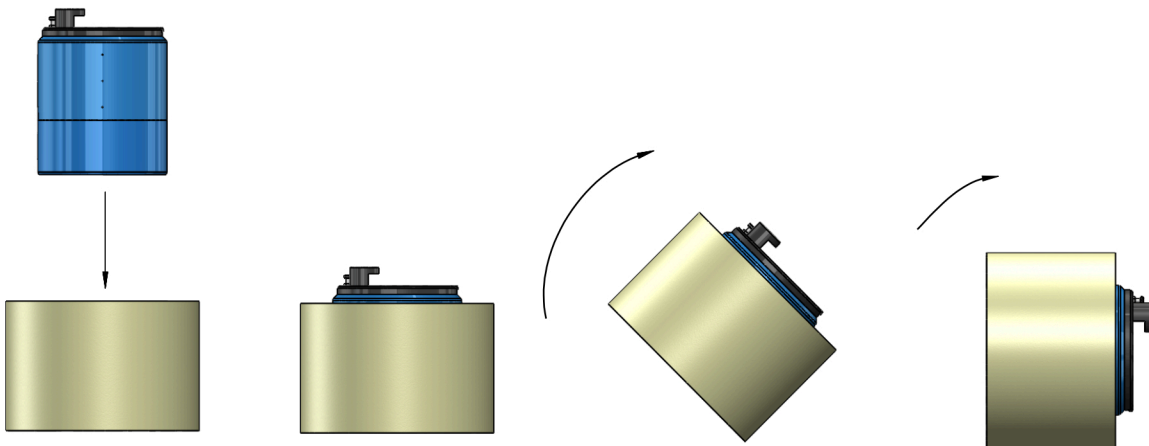
### Warning

The case mount should not be used with annuli that are 10cm thick or greater. When using these larger annuli the phantom and annuli should be placed on the patient couch.

If using 5cm thick annuli and the case mount, the case must be secured to the table by use of the patient restraint straps or additional counterweight. If the case is not secured to the table when the phantom is mounted, the case, phantom and annulus could fall off the edge of the table. Because the annuli add extra weight to the phantom check to see if the phantom is still level and adjust the leveling screw as required.



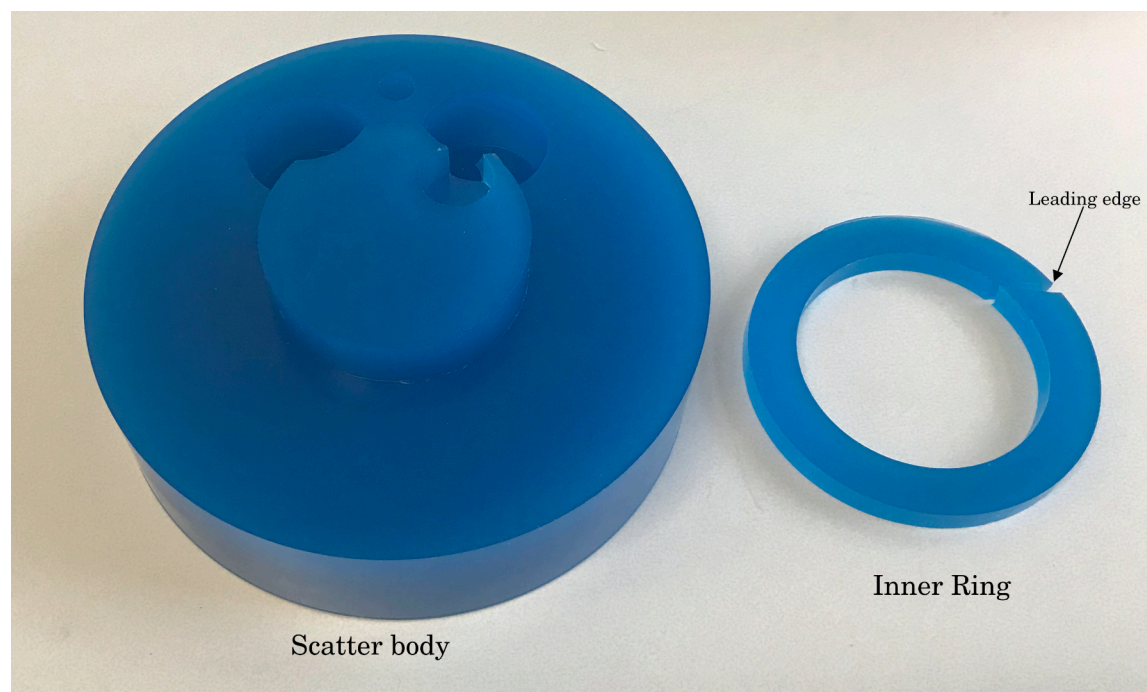
The Catphan 710 is supplied with two oval annuli, 25-35cm and 30-38cm in diameter with a 20cm length. For information on all the available Catphan® annuli sizes, go to our website library and download the “Catphan® Annuli Datasheet”



To mount, place the annulus on a flat side and lower the Catphan® phantom into the annulus. Then rotate the annulus and Catphan® phantom into the scanning position. Be careful to support the Catphan® while rotating so it does not slice out of position in the annulus.



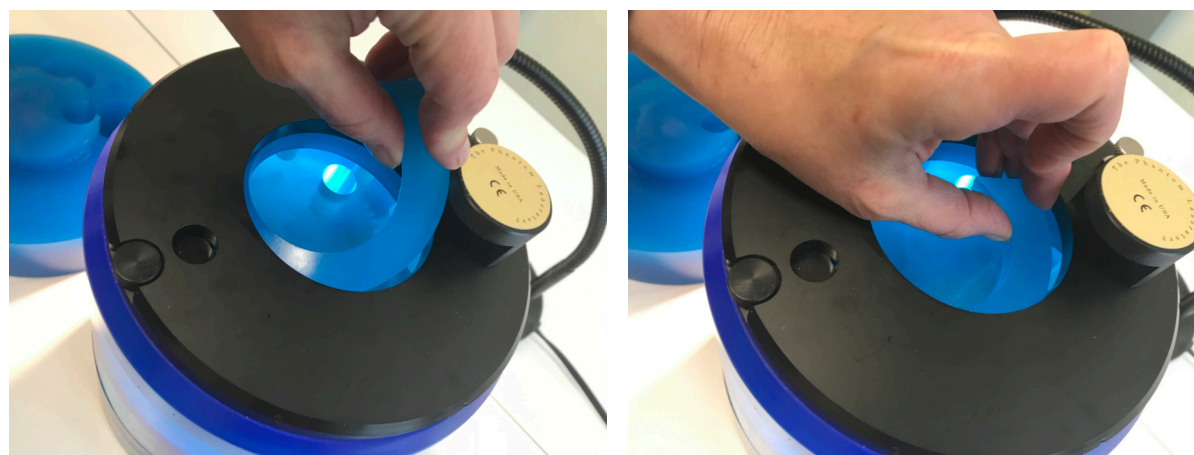
## Optional CCT285 Scatter Extension

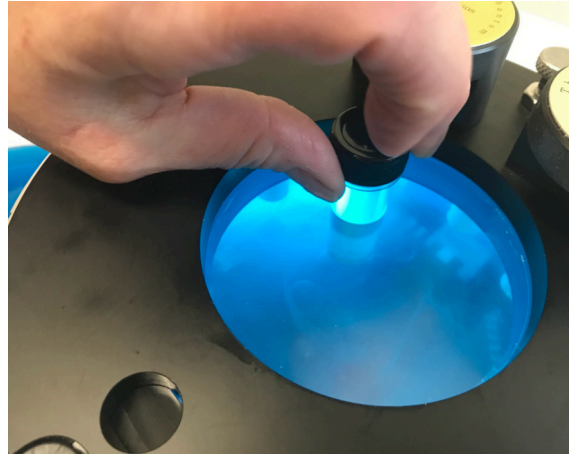


The optional CCT285 scatter extension is intended for use with cone beam or wide multi-slice CT scanners. It provides additional material on the front of the phantom to generate beam scatter through the CTP682 module. The case mount on the Catphan® 700 cannot be used with the scatter extension mounted. The Catphan® 700 with scatter extension either needs to be placed on the patient table or inside a 20cm long body annulus.

If your CCT285 scatter extension was purchased with a Catphan® 700, the inner ring may have already been installed at the factory.

To install the inner ring, remove the water vial, and then starting with the leading edge slide the ring into the gap between the Catphan® 700 mount and the CTP682 module. Once the ring is in place insert the water vial back into the CTP682 module.





After standing the Catphan® 700 on the uniformity end, the scatter body can be slid over the mount posts.

## Optional CTP748 High Density Insert Set



The High Density Insert Set is designed to be used with the CTP682 Module contained in a Catphan® 700.

These inserts enable repeatable comparisons between different CT systems and different protocols and post processing within a CT system regarding their ability to reduce streaking from high density materials.

The set contains 5 inserts:

1. Insert with 6.3 mm diameter titanium rod
2. Insert with 12.7 mm diameter titanium rod
3. Insert with 6.3 mm diameter stainless steel rod
4. Insert with 12.7 mm diameter stainless steel rod
5. Solid cast background urethane used as a control

Images of the CTP682 module with these inserts can be measured by the Smári Analysis service. The service records values in 5 defined regions of interest of the image containing streaking paths. In the Smári report the mean, standard deviation, and range are recorded for the 5 areas. By comparing this data, the effectiveness of streak reduction processing can be evaluated.

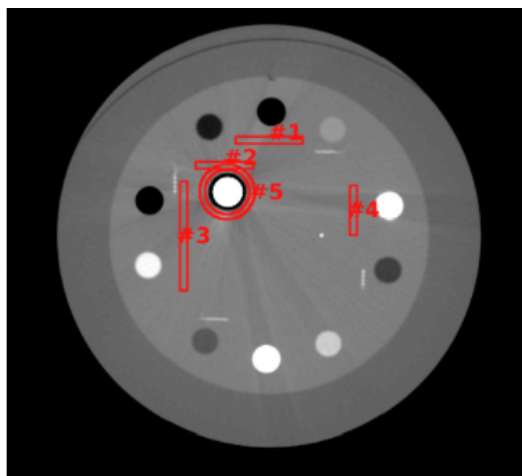


Image Number	Target size (small or large)	Max pixel value
4	Large	69

ROI#	Mean	SD	Range
ROI #1	58.0	2.77	16.0
ROI #2	58.6	2.65	15.0
ROI #3	59.1	2.66	17.0
ROI #4	58.0	2.88	18.0
ROI #5	58.6	2.88	19.0

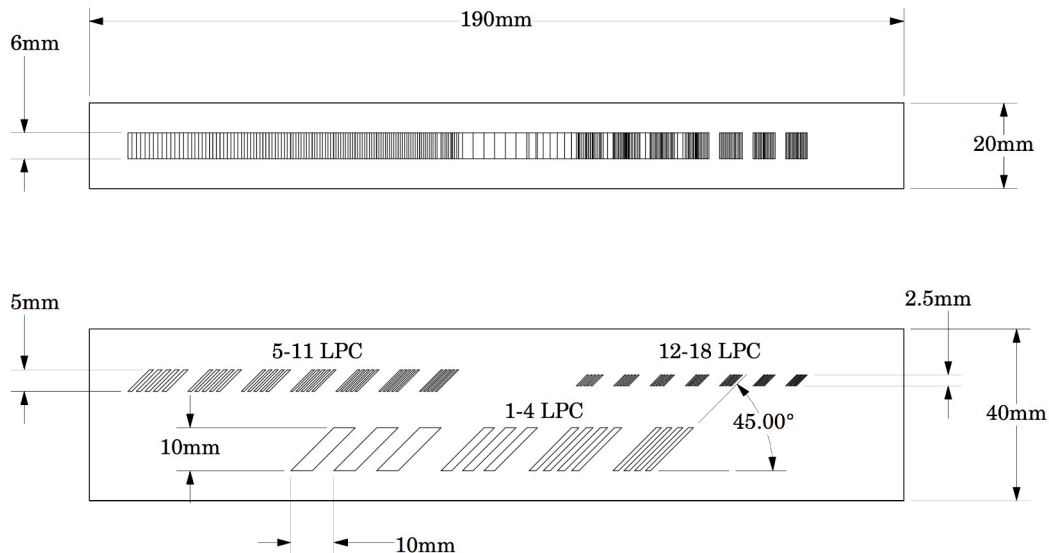


### Optional CCT287 45° High Resolution Phantom



The CCT287 45° High Resolution Phantom contains the patented 45° High Resolution Gauge that is designed to illustrate the 3-D volume resolution of a CT scanner at a specific imaging protocol. 3-D resolution is important when using CT for volume measurements or modeling such as radiation therapy treatment planning or building patient matched prosthetic devices. This can be used to evaluate the manufacturer's developments of greater isotropic resolution. Along with the gauge the phantom contains a 20cm diameter uniformity section.

Traditionally, we have measured 2-D resolution and then slice thickness or a slice sensitivity profile for the third dimension. The 45° Resolution Gauge provides a simple evaluation that reflects both of these measurements. This is very helpful when selecting protocols and trying to understand the influence of imaging protocols such as reconstruction filter, slice thickness and spiral pitch on the voxel size and precision.



The 45° Resolution Gauge contains 3 gauge sections in a 40mm x 190mm x 20mm clear urethane object. The contrast in the gauge is created by the aluminum bars set into the clear urethane. Based on the x direction, the gauge sections range from 1 to 18 line pair per centimeter LPCM. The bars are all set at a 45° angle from the axial slice plane.

## Bibliography

1. AAPM Report No. 39  
Specification and Acceptance Testing of Computed Tomography Scanners  
Report of Task Group 2 Diagnostic X-Ray Imaging Committee. Published for the American Association of Physicists in Medicine by the American Institute of Physics.  
May 1993
2. M. J. Berger, J. H. Hubbell, S. M. Seltzer, J. Chang, J. S. Coursey, R. Sukumar, and D. S. Zucker, Feb. 2009, XCOM: Photon Cross Sections Database, NIST Standard Reference Database 8 (XGAM), <http://www.nist.gov/physlab/data/xcom/index.cfm> (July 7, 2010).
3. Brooks and DiChiro  
Principles of Computer Assisted Tomography (CAT) in Radiographic and Radioisotopic Imaging  
Phys Med Biol 1976;21:689-732
4. Cohen and DiBanca  
The Use of Contrast-Detail-Dose Evaluation of Image Quality in a Computed Tomographic Scanner  
Comput. Assist. Tomogr. 3, 189-195 1979
5. Goodenough  
Volume Tomographic Imaging (Chapter 8)  
In: Bentel, Kundel, Van Metter (eds). Handbook of Medical Imaging, Volume 1: Progress in Medical Physics and Psychophysics.  
Bellingham, Washington, 2000: 511-554
6. Goodenough  
Assessment of Image Quality of Diagnostic Imaging Systems  
In: Gray GA (ed). Medical images: formation, perception and measurements. Proceedings of the 7th L.H.Gray Conference, New York: John Wiley & Sons, 1976:263-77
7. Goodenough  
Automated Quality Assurance for CT Scanners  
(Chapter): Radiology ICR 749, Editors Silver, Abecasis and Veiga-Pires. Excerpta Medica Press, Amsterdam 1987
8. Goodenough  
Psychophysical Perception of Computed Tomography Images  
In: Newton and Potts (eds). Radiology of the skull and brain: technical aspects of computed tomography. Vol 5, St. Louis: CV Mosby, 1981:3993-4021
9. Goodenough and Atkins  
Theoretical and Practical Aspects of Automated Quality Assurance Approaches, Particularly for CT  
Proceedings of the ICR 89, Excerpta Medica Press, Amsterdam 1990
10. Goodenough, Levy, and Kasales  
Development of Phantoms for Spiral CT  
Comput. Medical Imaging and Graphics 22 (1998) 247-255

11. Goodenough and Weaver  
Factors Related to Low Contrast Resolution in CT Scanners  
Computerized Radiology Vol. 8 No, 5. 279-308 1984
12. Goodenough, Weaver, and Davis  
Development of a Phantom for Evaluation and Assurance of Image Quality in CT Scanning  
The Proceedings of the Application of Optical Instrumentation in Medicine V meeting sponsored by  
The Society of Photo-Optical Instrumentation Engineers and The Society of Photographic Scientists  
and Engineers, September 16-19, 1976, Washington DC; and, Optical Engineering, January 1977
13. Goodenough, Weaver, and Davis  
Potential Artifacts Associated with the Scanning Pattern of the EMI Scanner  
Radiology 117:615-620, December 1975
14. Goodenough, Weaver, and Davis  
Physical Measurement of the EMI Imaging System  
In: Ter-Pogossian, Phelps, Brownell, Cos Jr., Davis and Evens (eds). Reconstruction tomography in  
diagnostic radiology and nuclear medicine. Baltimore: University Park Press, 1977: 225-243
15. John M. Boone and J. Anthony Seibert, 1997, An accurate method for computer-generating  
tungsten anode x-ray spectra from 30 to 140 kV, Medical Physics, v. 24, No. 11, p. 1661-1670.
16. R. J. Kriz and Keith J. Strauss, 1985, An investigation of computed tomography (CT) linearity,  
Medical Imaging and Instrumentation, v. 555, p. 195-204.
17. McCullough  
Photon Attenuation in Computed Tomography  
Medical Physics, 2:307-320, Nov/Dec 1975
18. McCullough, Baker, Hattery, Sheedy, Stephens and Payne  
Performance Evaluation and Quality Assurance of Computed Tomography (CT)  
Equipment with Illustrative Data for ACTA, Delta , and EMI Scanners  
Radiology 120: 173-188, July 1976
19. McCullough, Baker, Houser, and Reese  
An Evaluation of the Quantitative and Radiation Features of Scanning X-ray Transverse Axial  
Tomography: the EMI Scanner  
Radiology 111: 709-715, June 1974
20. Phelps, Hoffmar-Pogossian  
Attenuation Coefficients of Various Body Tissues, Fluids and Lesions at Photon Energies of 18 to 136  
keV  
Radiology 117:573-583, December 1975
21. Rossmann  
Point Spread Function, Line Spread Function and Modulation Transfer Function: Tools for the Study  
of Imaging Systems  
Radiology 1969:93:257-72
22. T. R. Fewell, R. E. Shuping, and K. E. Healy, 1981, Handbook of Computed Tomography X-ray  
Spectra, HHS Publication (FDA) 81-8162 (U.S. Government Printing Office, Washington D.C.).

23. Weaver, Goodenough, and Briefel  
Sensitometry in Computerized Tomography  
Proceedings of SPIE, Medicine VI. 1977:127:87-94

24. Yester and Barnes  
Geometrical Limitations of Computed Tomography (CT) Scanner Resolution  
Optical instrumentation in Medicine VI. SPIE, 1977:127:296-303

